The EMBO Journal (2012) 31, 4106–4123 | © 2012 European Molecular Biology Organization | Some Rights Reserved 0261-4189/12
www.embojournal.org

THE EMBO JOURNAL

EMBO open

Upregulated function of mitochondria-associated ER membranes in Alzheimer disease

Estela Area-Gomez[1], Maria del Carmen Lara Castillo[1], Marc D Tambini[2], Cristina Guardia-Laguarta[3], Ad JC de Groof[1,4,9], Moneek Madra[5], Junichi Ikenouchi[6], Masato Umeda[6], Thomas D Bird[7], Stephen L Sturley[5] and Eric A Schon[1,8,*]

[1]Department of Neurology, Columbia University Medical Center, New York, NY, USA, [2]Department of Cellular, Molecular and Biophysical Studies, Columbia University Medical Center, New York, NY, USA, [3]Department of Pathology and Cell Biology, Columbia University Medical Center, New York, NY, USA, [4]Department of Cell Biology, NCMLS, Radboud University, Nijmegen, The Netherlands, [5]Department of Pediatrics, Columbia University Medical Center, New York, NY, USA, [6]Department of Synthetic Chemistry and Biological Chemistry, Kyoto University, Kyoto, Japan, [7]Division of Neurogenetics, University of Washington and Geriatrics Research Center, VA Medical Center, Seattle, WA, USA and [8]Department of Genetics and Development, Columbia University Medical Center, New York, NY, USA

Alzheimer disease (AD) is associated with aberrant processing of the amyloid precursor protein (APP) by γ-secretase, via an unknown mechanism. We recently showed that presenilin-1 and -2, the catalytic components of γ-secretase, and γ-secretase activity itself, are highly enriched in a subcompartment of the endoplasmic reticulum (ER) that is physically and biochemically connected to mitochondria, called mitochondria-associated ER membranes (MAMs). We now show that MAM function and ER–mitochondrial communication—as measured by cholesteryl ester and phospholipid synthesis, respectively—are increased significantly in presenilin-mutant cells and in fibroblasts from patients with both the familial and sporadic forms of AD. We also show that MAM is an intracellular detergent-resistant lipid raft (LR)-like domain, consistent with the known presence of presenilins and γ-secretase activity in rafts. These findings may help explain not only the aberrant APP processing but also a number of other biochemical features of AD, including altered lipid metabolism and calcium homeostasis. We propose that upregulated MAM function at the ER–mitochondrial interface, and increased cross-talk between these two organelles, may play a hitherto unrecognized role in the pathogenesis of AD.
The EMBO Journal (2012) **31,** 4106–4123. doi:10.1038/emboj.2012.202; Published online 14 August 2012
Subject Categories: membranes & transport; neuroscience
Keywords: APP; cholesterol; MAM; phospholipids; presenilin

*Corresponding author. Department of Neurology, Columbia University Medical Center, Room P&S 4-449, 630 West 168th Street, New York, NY 10032, USA. Tel.: +1 212 305 1665; Fax: +1 212 305 3986; E-mail: eas3@columbia.edu
[9]Present address: Merck/Intervet International bv, Wim de Körverstraat 35, PO Box 31, 5830 AA Boxmeer, The Netherlands

Received: 16 January 2012; accepted: 28 June 2012; published online: 14 August 2012

Introduction

Alzheimer disease (AD) is a late onset neurodegenerative disorder characterized by progressive neuronal loss, especially in the cortex and the hippocampus (Goedert and Spillantini, 2006). The vast majority of AD is sporadic (SAD), but mutations in the amyloid precursor protein (APP) and in presenilin-1 (PS1) and -2 (PS2), which are components of the γ-secretase complex that processes APP to produce amyloid-β (Aβ), have been identified in the familial form (FAD), which is similar to SAD but has an earlier age of onset. To date, there is no unifying hypothesis that can explain the diverse and apparently unrelated morphological and biochemical abnormalities—extracellular plaques containing Aβ fibrils (Pimplikar, 2009), intracellular tangles containing hyperphosphorylated forms of the microtubule-associated protein tau (Pimplikar, 2009), elevated serum cholesterol (Stefani and Liguri, 2009), altered phospholipid metabolism (Wells *et al*, 1995; Pettegrew *et al*, 2001), aberrant calcium homeostasis (Bezprozvanny and Mattson, 2008), and mitochondrial dysfunction (Wang *et al*, 2009)—detected in tissues and in cultured cells from AD patients (Pimplikar, 2009), with no apparent direct link among them.

In the case of FAD, investigations into a common source of these apparently unrelated features have been complicated by uncertainty regarding the subcellular distribution of the presenilins. PS1 and PS2 have been located to numerous subcellular compartments, including endoplasmic reticulum (ER) (Annaert *et al*, 1999), Golgi (Annaert *et al*, 1999), plasma membrane (PM) (Marambaud *et al*, 2002), nuclear envelope (Kimura *et al*, 2001), endosomes (Vetrivel *et al*, 2004), lysosomes (Pasternak *et al*, 2003), and mitochondria (Ankarcrona and Hultenby, 2002). On the other hand, it is generally accepted that APP (Kosicek *et al*, 2010), presenilins, Aβ, and γ-secretase activity are enriched in lipid rafts (LRs) (Urano *et al*, 2005; Vetrivel *et al*, 2005), which are specialized domains rich in cholesterol and sphingolipids that form detergent-insoluble aggregates in cell membranes (i.e., detergent-resistant membranes, or DRMs) (Simons and Vaz, 2004). These regions have a liquid-ordered structure with unique biophysical characteristics that differs from the rest of the cell's liquid-disordered membranes (Simons and Vaz, 2004). Traditionally, LRs have been considered to be present only in the PM (Simons and Vaz, 2004). However, γ-secretase activity is negligible in this compartment, forming the basis of what has been called 'the spatial paradox' (Cupers *et al*, 2001). Recent evidence, however, has in fact indicated the existence of intracellular LRs/DRMs that are different in protein composition from those in the PM (Browman *et al*, 2006).

We recently found that PS1, PS2, APP, and γ-secretase activity are not homogeneously distributed in the ER, but rather are enriched in mitochondria-associated ER membranes (ER-MAMs or MAMs) (Area-Gomez *et al*, 2009). MAM is a dynamic subcompartment of the ER connected

physically and biochemically to mitochondria that is involved in a number of key metabolic functions (Hayashi *et al*, 2009), including cholesterol metabolism (Rusinol *et al*, 1994), the synthesis and transfer of phospholipids between the ER and mitochondria (Vance, 2003), and calcium homeostasis (Csordas *et al*, 2010).

We now report that MAM is a complex elaboration of the ER with the characteristics of an LR. Moreover, using a number of relevant tissues and cell lines (Supplementary Table S1), we show that mutations in presenilins perturb MAM function significantly, and that these perturbations are also present in cells from FAD patients with mutations in PS1, PS2, and APP, and in SAD patients with no known genetic aetiology. These findings may shed new light on the biology of presenilins and on our understanding of some of the features associated with the pathogenesis of AD.

Results

MAM displays the characteristics of an intracellular LR

MAM is a dynamic domain of the ER responsible for the integration of several cellular functions, including Ca^{2+} signalling, lipid transport, energy metabolism, and cellular survival. For this reason, we speculated that MAM might have the characteristics of an LR/DRM in order for it to recruit and orientate the different signalling proteins needed for cellular homeostasis and for the effective cross-talk between mitochondria and ER (Hayashi and Fujimoto, 2010; Williamson *et al*, 2011; Fujimoto *et al*, 2012). In addition, the fact that γ-secretase activity is present in LRs (Vetrivel *et al*, 2005) and is also enriched in MAM (Area-Gomez *et al*, 2009) provided indirect support for the idea that MAM could be an LR/DRM.

We therefore incubated purified MAM from mouse tissues (Area-Gomez *et al*, 2009; Supplementary Figure S1) with and without Triton X-100 (TX100), and loaded both samples onto a Percoll gradient under the same conditions used for its initial isolation. The TX100-treated MAM sample was fundamentally intact and migrated to the identical position in the gradient as did the untreated sample, consistent with the behaviour of a DRM (Figure 1A). To separate LR from other cell contents, we loaded TX100-treated and untreated control MAM from mouse brain onto a sucrose gradient, and analysed fractions for the known MAM markers Pemt (phosphatidylethanolamine *N*-methyltransferase; Vance, 1990), Vdac1 (voltage-dependent anion channel 1; Hayashi *et al*, 2009), and Ps1 (Area-Gomez *et al*, 2009; Figure 1B). The proteins migrated at similar positions in the lower density fractions, and were unaffected by detergent treatment (Figure 1B), consistent with the behaviour of MAM as a DRM. By contrast, purified mitochondria and bulk ER from the bottom of the gradient behaved like detergent-soluble fractions (Supplementary Figure S2), indicating the absence of DRMs in these organelles, as expected (Zheng *et al*, 2009). MAM was not contaminated with PM rafts, as Src, a marker for PM rafts (Morrow and Parton, 2005), was observable in sucrose gradient fractions from purified PM, but not from the crude mitochondrial fraction from which the MAM fraction was derived (Figure 1C). Moreover, the cholesterol content of MAM was higher than that found in the cytoplasm, mitochondria, bulk ER, and total PM, and was comparable to that of LR from PM (Simons and Vaz, 2004; Figure 2A). These

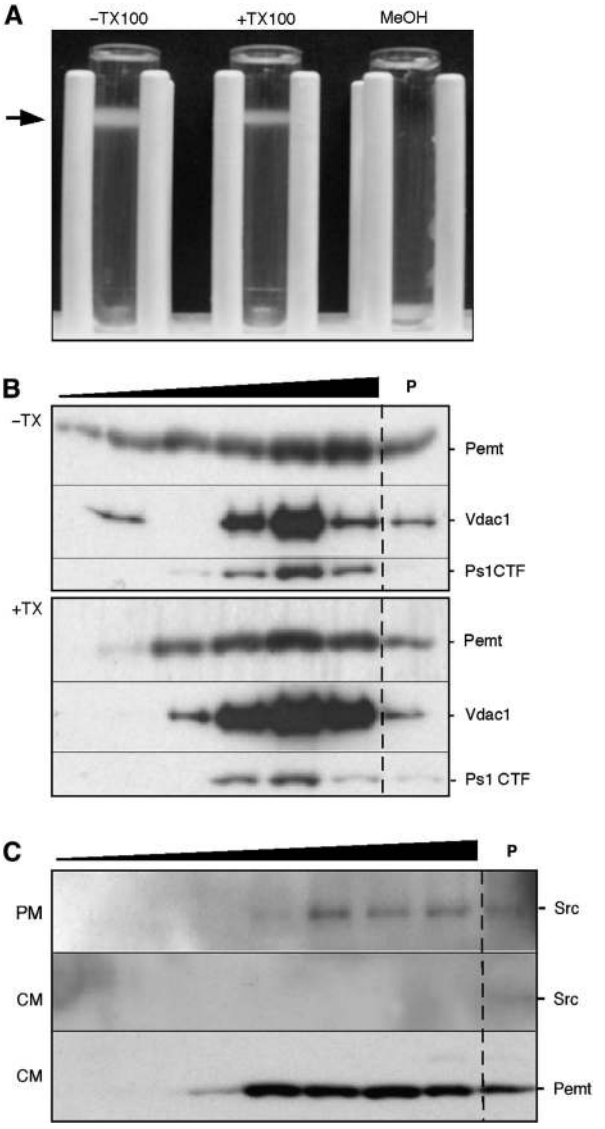

Figure 1 MAM displays the features of a lipid raft. (**A**) Mouse liver Percoll-purified MAM treated with or without TX100 prior to centrifugation through a second Percoll gradient. The low density fraction (arrow) is detergent resistant but solubilizable by methanol (MeOH), implying that it is a DRM. (**B**) Western blot of fractions from a 5–30% sucrose gradient (triangle; lower density at left) of MAM isolated from a Percoll gradient (as in **A**). The pellet (P) denotes TX100-soluble material. (**C**) Western blot of gradient fractions of mouse liver PM and crude mitochondrial extract (CM) to detect Src (PM marker) and Pemt (MAM marker).

results are consistent with the numerous reports showing that presenilins and γ-secretase activity reside in LRs and suggest that MAM is an intracellular LR-like domain that may recruit and orient various signalling proteins needed to regulate cross-talk between ER and mitochondria.

Elevated cholesteryl ester synthesis in PS-mutant cells and AD patient fibroblasts

Given that MAM is an LR/DRM, the regulation of cholesterol metabolism should be an important determinant of its structure and function. Acyl-CoA:cholesterol acyltransferase (ACAT), which catalyses the conversion of free cholesterol to cholesteryl esters (CE) and controls the equilibrium between membrane-bound free cholesterol and CE stored in

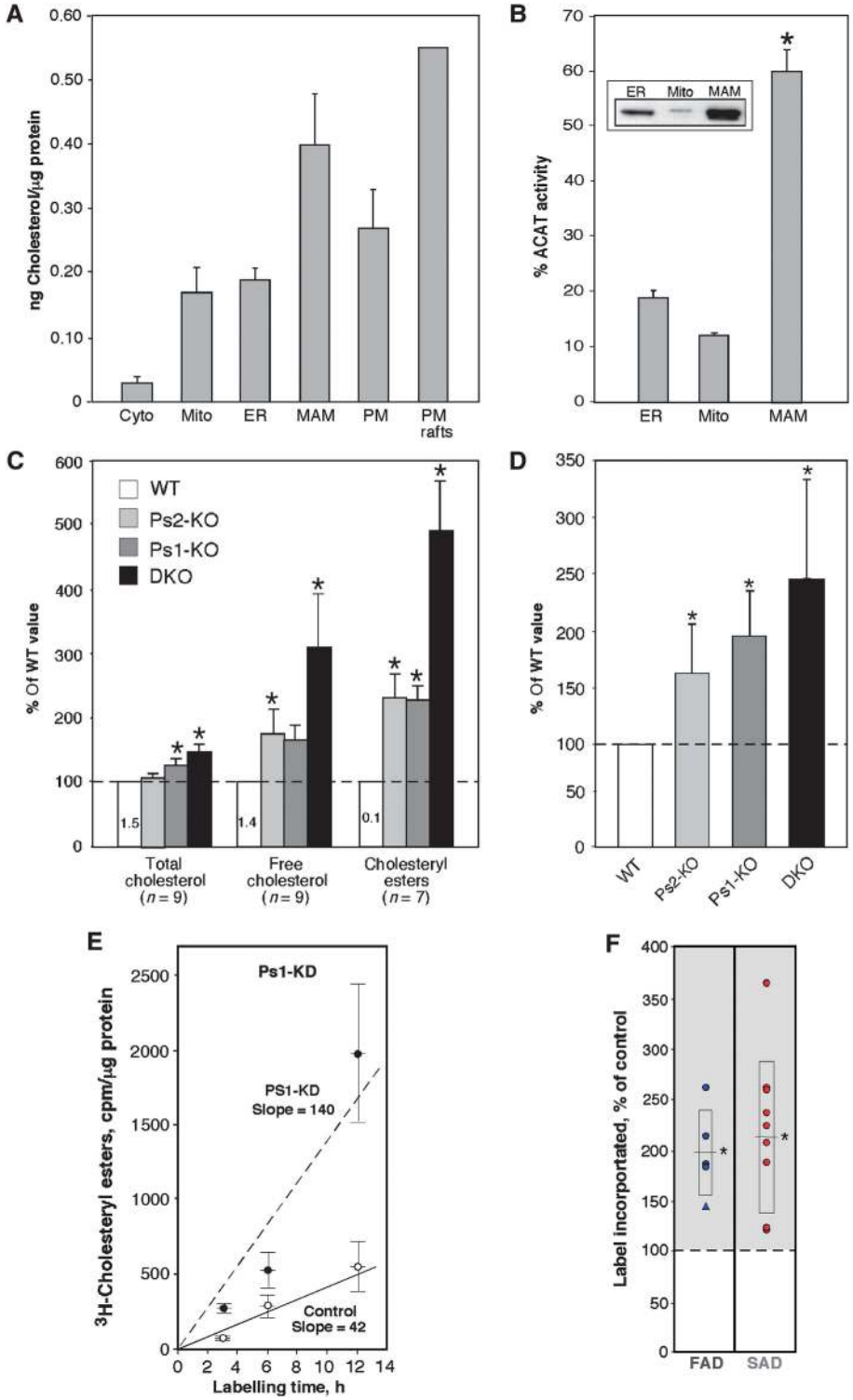

Figure 2 Cholesterol metabolism in PS-mutant and AD cells. (**A**) Total cholesterol in the indicated mouse brain fractions ($n = 3$, except PM rafts; $n = 2$). (**B**) ACAT activity in mouse brain fractions ($n = 4$). Inset: western blot to detect ACAT protein; 20 μg protein loaded in each lane. Asterisk denotes significant difference versus ER and mito fractions ($P < 0.05$). (**C**) Content of cholesterol species in PS-mutant MEFs relative to that in WT MEFs (numbers denote average amounts of the indicated cholesterol species, in ng/mg protein). (**D**) ACAT activity (i.e., conversion of ^{3}H-cholesterol to ^{3}H-cholesteryl esters) in MEFs after 6 h ($n = 6$). (**E**) Kinetics of CE synthesis (performed as in **D**) in Ps1-KD cells (note increased slope (line of best fit, in cpm/μg/h) versus control). (**F**) Quantitation of ^{3}H-CE synthesis after 6 h in fibroblasts from FAD ($n = 5$; 4 PS1 (circles), 1 PS2 (triangle)) and SAD ($n = 9$) patients versus paired controls. For cell lines that were evaluated multiple times (see Supplementary Table S1), the data point represents an average of the assays. Boxes with centred lines denote averages ± s.d.; asterisks denote significant difference versus WT ($P < 0.05$).

cytoplasmic lipid droplets (Puglielli *et al*, 2001), is enriched in MAM (Rusinol *et al*, 1994). We confirmed that MAM is indeed the predominant locus for CE synthesis, as ACAT protein was not only more abundant in MAM as compared to bulk ER and mitochondria (Figure 2B, inset), but also had an ~3-fold higher enzymatic activity (Figure 2B).

Using CE synthesis as a probe of MAM function, we determined the role of presenilins in this process by analysing mouse embryonic fibroblasts (MEFs) lacking Ps1 (Ps1-KO), Ps2 (Ps2-KO), or both proteins (DKO). Compared to wild-type (WT) MEFs, the mutant lines showed increased steady-state levels of total (Grimm *et al*, 2005) and free cholesterol (Figure 2C), but more importantly, the relative differences in CE content were even greater, with up to ~5-fold more CE in DKO than in WT MEFs (Figure 2C). Upon labelling the cells with ^{3}H-cholesterol to monitor its conversion by ACAT into ^{3}H-cholesteryl esters, we found significantly higher ACAT activity in the Ps-mutant MEFs (up to ~2.5-fold over controls) (Figure 2D). Both presenilin isoforms contributed to CE synthesis, as the average increase in CE content was far more pronounced in the Ps1 + Ps2 DKO MEFs (145% greater than WT) than in either individual knockout alone (96 and 63% greater than WT in Ps1- and Ps2-KO, respectively) (Figure 2D). In a control experiment, we determined that this upregulation was not due to an increase in *Acat1* expression (Supplementary Figure S3). Because CE synthesis in the Ps1-KO cells was higher than in the Ps2-KOs, and because PS1 plays a more significant role in FAD than does PS2 (Jayadev *et al*, 2010), we also examined CE synthesis in immortalized mouse MEFs in which Ps1 expression had been knocked down (Ps1-KD) (Supplementary Figure S4). There was an ~3-fold increase in the kinetics of CE formation in Ps1-KD cells versus control (Figure 2E). Notably, we detected significant increases in CE synthesis in PS-mutant FAD cells (~1.8-fold higher than controls), and equally strikingly, in SAD cells as well (~1.7-fold higher) (Figure 2F).

Consistent with the increase in CE, we observed numerous structures that appeared to be lipid droplets in electron microscopic images of DKO, but not control, MEFs (asterisks in Figure 3A). We therefore looked for the presence of lipid droplets after staining cells with HCS LipidTox Green^{TM} (Figure 3B) and Oil Red O (Supplementary Figure S5). Whereas the LipidTox stain in WT MEFs was diffuse, the PS-mutant MEFs contained numerous discrete LipidTox-positive droplets (~5-fold greater signal) (Figure 3B; see also Supplementary Figure S6). Similar results were also obtained with the Ps1-KD cells (Figure 3C); importantly, the increase in lipid droplets in Ps1-KD cells (~5-fold over control) was rescued by overexpression of human WT PS1, but not of human PS1 harbouring the A246E mutation found in many FAD patients (Figure 3C). Notably, we detected significantly more lipid droplets in fibroblasts from FAD patients (with mutations in PS1, PS2, and APP) and in SAD fibroblasts (an average of ~20–30% of the cells was LipidTox positive) versus controls (~3% positive) (Figure 3D; Supplementary Figures S5 and S6). These observations may help explain the elevated numbers of lipids droplets found in fibroblasts (Pani *et al*, 2009a) and neurons (Gómez-Ramos and Asunción Morán, 2007) of SAD patients.

Taken together, the data indicate that MAM activity, as measured by CE synthesis, is altered in AD, and that presenilins and APP, and perhaps also γ-secretase activity, may play a key role in regulating MAM function.

Elevated phospholipid synthesis in PS-mutant cells and AD patient fibroblasts

It is well known that ER–mitochondrial communication via MAM is necessary for phospholipid synthesis (Voelker, 2005). Phosphatidylserine (PtdSer) is synthesized in the MAM (Hayashi *et al*, 2009); it then translocates to mitochondria, where it is converted to phosphatidylethanolamine (PtdEtn); PtdEtn then translocates back to the MAM, where it is methylated (by PEMT) (Vance, 2008) to generate phosphatidylcholine (PtdCho). The trafficking of these phospholipids between ER and mitochondria is a recognized measure of the communication between both organelles and of the regulation of MAM function (Voelker, 2005). Therefore, to test directly the role of presenilins in ER–mitochondrial communication, we incubated Ps-mutant MEFs in medium containing ^{3}H-serine (^{3}H-Ser) and measured the incorporation of the label into newly synthesized ^{3}H-PtdSer and ^{3}H-PtdEtn. The levels of both labelled species increased >3-fold in the DKO MEFs as compared to WT (Figure 4A), suggesting an upregulation of MAM function and of ER–mitochondrial cross-talk in these cells. In a control experiment, we determined that this upregulation was not due to an increase in the expression of *Ptdss1*, *Ptdss2*, or *Pisd*, three key genes involved in transport of phospholipids between ER and mitochondria (Supplementary Figure S3).

To determine the kinetics of this upregulation, we performed pulse-chase analysis by incubating the MEFs with ^{3}H-Ser for 1 h, followed by a chase with cold serine for various time periods (Figure 4B). The incorporation of label into ^{3}H-PtdSer during the pulse (time 0 in Figure 4B) was significantly higher in the Ps1-KO and DKO MEFs than in control. During the chase, the amount of ^{3}H-PtdSer decreased and that of ^{3}H-PtdEtn increased, consistent with the conversion of the former into the latter, with higher rates in the Ps1-KO and DKO MEFs (up to three-fold higher). While the increase in lipid synthesis in the pulse-chase was not altered significantly in the Ps2-KO MEFs, Ps2 clearly contributes to phospholipid metabolism and MAM function, as lipid synthesis in the Ps1 + Ps2 double knockout was much more pronounced than in the Ps1-knockout alone (Figure 4B). These results were confirmed in isolated MEF crude mitochondrial fractions (containing essentially only ER, MAM, and mitochondria; Area-Gomez *et al*, 2009) (Figure 4C). The rate of phospholipid synthesis was also increased in Ps1-KD cells (Figure 4D) and, importantly, in FAD and SAD fibroblasts (by ~1.5- to 2-fold over controls) (Figure 4E).

Since some of the PtdEtn synthesized is exported to the inner leaflet of the PM (Vance, 2008), we hypothesized that it would be elevated in the PM of mutant cells. Accordingly, we treated cells with two highly related antibiotics, cinnamycin (Cin; also called Ro09-0198) (Choung *et al*, 1988) and duramycin (Dura) (Marki *et al*, 1991), both of which are 19-aa cyclic peptides that form a complex specifically with PtdEtn to induce pore formation in the PM in a PtdEtn concentration-dependent manner, followed by rapid cell death (Makino *et al*, 2003) (see example in Figure 5A, left and middle panels). Ps1-KO and DKO MEFs were ~3.5-fold more Cin sensitive than were controls (Figure 5A, right panel). Similarly, Ps1-KD cells were ~3-fold more Cin sensi-

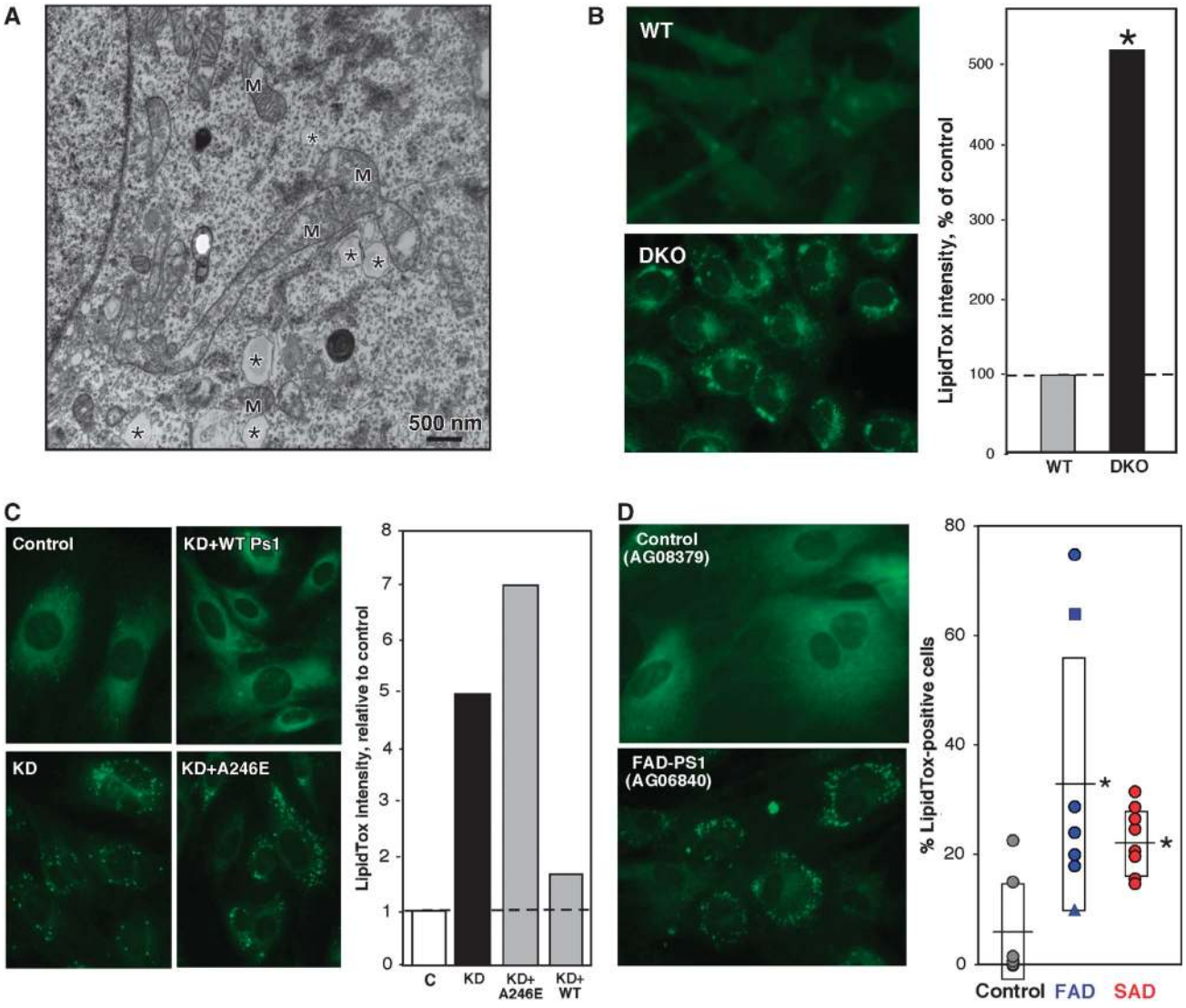

Figure 3 Detection of lipid droplets in PS-mutant and AD cells. (**A**) EM of DKO MEFs. Note the presence of features reminiscent of lipid droplets (asterisks); these were not observed in WT MEFs. M, mitochondrion. (**B**) Left: LipidTox staining of DKO MEFs; note punctate staining (i.e., lipid droplets) that are absent in WT MEFs. Right: Quantitation of LipidTox staining. (**C**) Left: LipidTox staining of Ps1-KD cells. Right: Quantitation, as in (**B**). Note that overexpression of human WT-PS1, but not A246E mutant PS1, reduced lipid droplet formation. C, mismatched shRNA control. (**D**) Example of LipidTox staining (left) and quantitation of LipidTox-positive fibroblasts from FAD ($n=7$) and SAD ($n=9$; 7 PS1 (circles), 1 PS2 (triangle), 1 APP (square)) patients versus controls ($n=7$) (right). See other examples in Supplementary Figure S6. Other notation as in Figure 2.

tive than were controls; as before, this sensitivity could be rescued by overexpression of human WT, but not A246E mutant, PS1 (Figure 5B, left panel). Notably, FAD and SAD cells were significantly (~3- to 5-fold) more Cin sensitive than were controls (Figure 5B, right panel). We also were able to visualize the presence of PtdEtn on the cell surface by staining cells with FL-SA-Ro (Figure 5C), a fluorescent-conjugated form of cinnamycin that binds to PtdEtn on the PM but does not initiate cell death (Emoto *et al*, 1996). In agreement with the Cin-sensitivity results, ~4 times as many FAD and SAD cells were stained with FL-SA-Ro as compared to controls (Figure 5C; Supplementary Figure S7).

Together with the CE data, these results point to an upregulation of MAM function in AD, either by mutations in presenilins or APP or, in the case of SAD, by unknown causes.

Increased ER–mitochondrial contacts in PS-mutant cells and AD patient fibroblasts

The increased biochemical activity of MAM in PS-mutant cells prompted us to see if ER–mitochondrial contacts were physically altered. We therefore transfected cells with DsRed-Mito to detect mitochondria (in red) and with GFP-Sec61β to detect ER (in green), and used confocal microscopy and Image J analysis to detect and quantitate regions where the two signals were in close apposition (see example in Figure 6A). Using this method, we found that the degree of ER–mitochondrial apposition was significantly higher in Ps1-KO (~34 ± 10% of the total signal), Ps2-KO (34 ± 6%), and DKO (56 ± 6%) MEFS than in WT MEFS (12 ± 4%) (Figure 6B, left). Moreover, the degree of apposition was significantly higher in fibroblasts from both FAD (26 ± 4%) and SAD (24 ± 6%) patients than in those from controls (11 ± 2%) (Figure 6B, right).

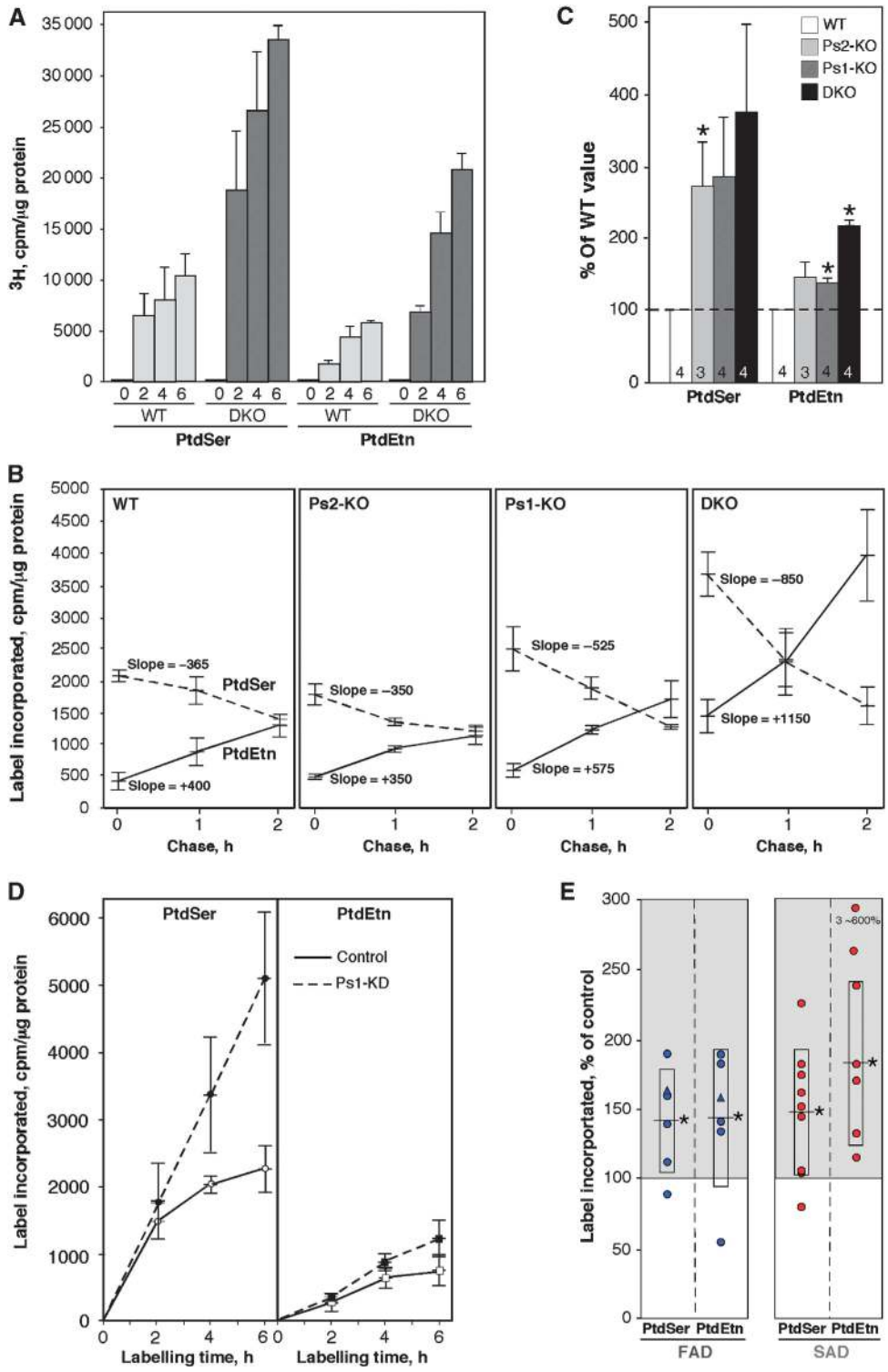

Figure 4 Phospholipid synthesis in PS-mutant and AD cells. (**A**) Synthesis of ^{3}H-PtdSer and ^{3}H-PtdEtn after labelling DKO MEFs with ^{3}H-Ser for the indicated times (h) ($n=3$). (**B**) Pulse-chase. MEFs were labelled for 1 h with ^{3}H-Ser and chased with cold Ser for the indicated times ($n=3$). Note the steeper slopes (i.e., rates of ^{3}H-Ser incorporation) for both PtdSer (negative slopes) and PtdEtn (positive slopes), indicative of a more rapid conversion of PtdSer to PtdEtn, especially in the DKO cells. (**C**) Phospholipid synthesis in crude mitochondria from Ps-KO MEFs ($n=3$ or 4, as indicated; error bars, s.e.). (**D**) Kinetics of PtdSer and PtdEtn synthesis (as in **A**) in Ps1-KD cells. (**E**) Phospholipid synthesis after 6 h (as in **A**) in fibroblasts from FAD ($n=6$) and SAD ($n=9$) patients. Note: three of the SAD PtdEtn values were unusually high (~600% of control) and were omitted from the statistical analyses. Other notation as in Figure 2.

In order to observe ER–mitochondrial apposition at higher resolution, we imaged MEFs and patient cells by electron microscopy (EM). We observed a significant increase in the length of mitochondrial-ER contacts (i.e., MAM) in DKO as compared to WT MEFs (Figure 7). Specifically, there were significantly more numerous 'long' (50–200 nm; Figure 7C) and 'very long' (>200 nm; Figure 7E) contacts in DKO MEFs than in WT MEFs (~5-fold and >10-fold, respectively;

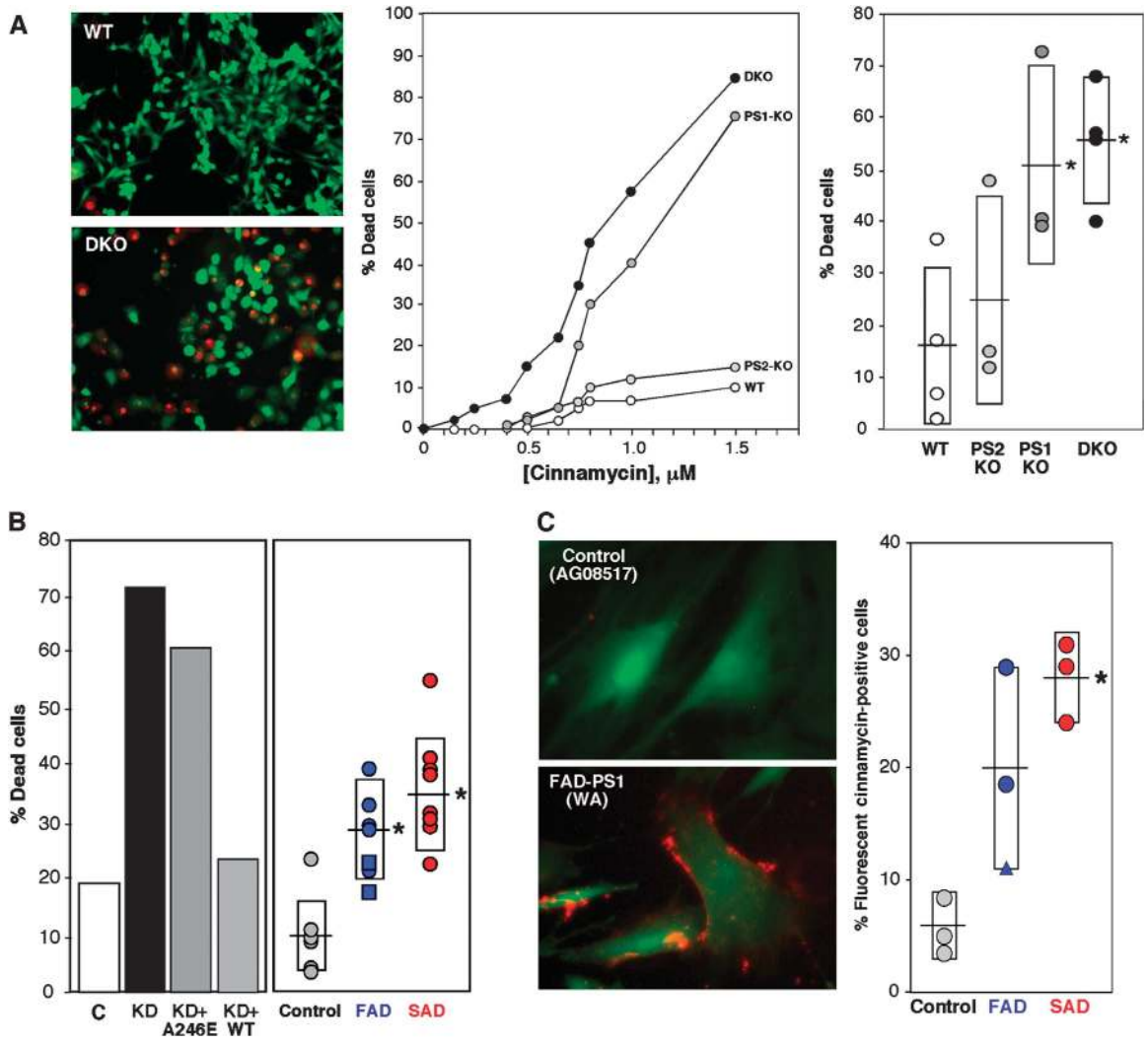

Figure 5 Cinnamycin sensitivity in PS-mutant and AD cells. (**A**) Left: Example of live/dead assays (1 μM cinnamycin for 10 min at 37°C). Middle: Example of cinnamycin-sensitivity curves in PS-mutant MEFs. Right: Summary of cinnamycin sensitivity assays (1 μM Cin for 10 min) in PS-mutant MEFs. (**B**) Left: Example of cinnamycin sensitivity in Ps1-KD cells versus mismatch control (C). Note that overexpression of human WT PS1, but not A246E mutant PS1, could 'rescue' Cin sensitivity. Right: Cin/Dura sensitivity in fibroblasts from FAD ($n=7$) and SAD ($n=8$) patients versus controls ($n=7$). (**C**) Left: Example of staining of control and AD patient cells with fluorescent cinnamycin (FL-SA-Ro; orange); cells were counterstained with calcein (green) to visualize overall cell morphology. Right: Quantitation of FL-SA-Ro staining in fibroblasts from FAD ($n=3$) and SAD ($n=3$) patients compared to controls ($n=3$). See other examples in Supplementary Figure S7. Other notations as in Figures 2 and 3.

Figure 7F, left), whereas connections in WT MEFs were much shorter and more 'punctate' (<50 nm; Figure 7B). We found a similar increase in 'long' and 'very long' contacts in AD patients (Figure 7F, right; Supplementary Figure S8). Thus, the increased biochemical activity of MAM in PS-mutant and in AD cells correlated with an increased area of physical association between the two organelles.

Analysis of MAM function in cells deficient in ER–mitochondrial communication

If upregulated MAM function in PS-mutant and AD cells is related to increased ER–mitochondrial communication, then decreased contacts between the two organelles should have an opposite effect. We therefore assayed cholesterol ester and phospholipid synthesis in MEFs lacking mitofusin-2 (Mfn2), a protein that is required for MAM-mediated ER–mitochondrial interactions (de Brito and Scorrano, 2008). In agreement with our hypothesis, we found an ~2-fold lower rate of CE synthesis in Mfn2-KO MEFs (Figure 8A), and an ~25% decrease in phospholipid synthesis and transport, as compared to WT MEFs (Figure 8B). Finally, we asked whether the deficient ER–mitochondrial communication present in Mfn2-KO cells affected γ-secretase activity. We measured the levels of APP and its C-terminal cleavage products C99 and AICD (APP intracellular domain) (Area-Gomez *et al*, 2009; Flammang *et al*, 2012) (see scheme in Figure 8C). There was an ~2-fold reduction in the amount of AICD in Mfn2-KO cells as compared to WT, and a concomitant increase in C99 (Figure 8C). As a control, we also measured these three proteins in WT and DKO MEFs. As expected, no AICD was produced in the DKO cells (Area-Gomez *et al*, 2009), while C99 accumulated accordingly (Figure 8C). Importantly, the reduction in γ-secretase activity in Mfn2-KO cells was not due to a relocalization or mislocalization of presenilins in these

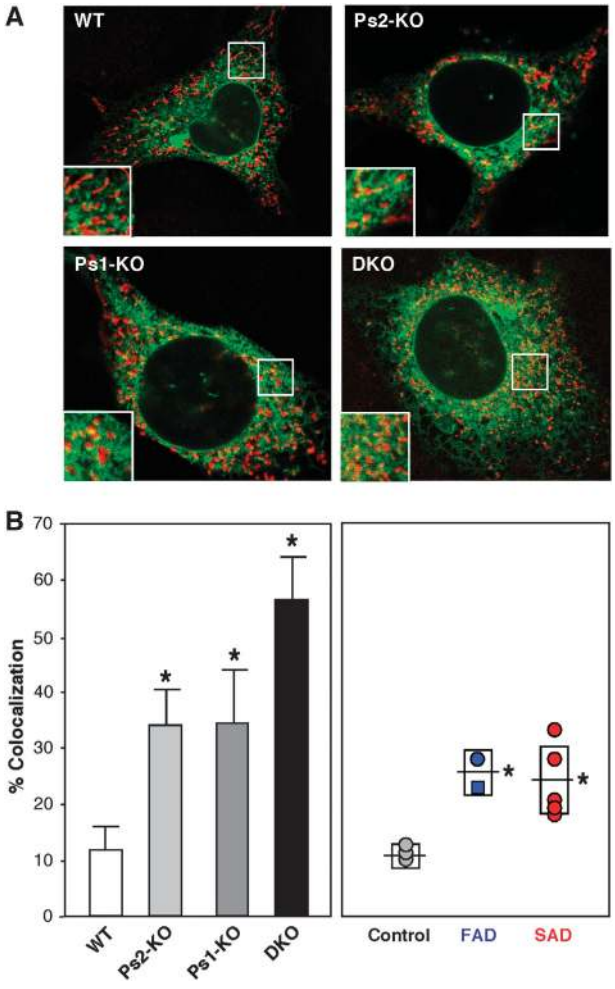

Figure 6 ER–mitochondrial colocalization in Ps-mutant and AD cells. (**A**) Example of confocal images of cells stained with Mito DS Red (red) and GFP-Sec61β (green). In the insets, note the large number of discrete red and green signals in the WT as compared to the Ps-mutant MEFs, which have more overlap (orange and yellow signals). (**B**) Quantitation of colocalization (as in **A**) by Image J in WT (average of 10 images ± s.d.), Ps1-KO ($n=11$), Ps2-KO ($n=13$), and DKO ($n=7$) MEFs (left), and in fibroblasts from FAD ($n=2$) and SAD ($n=5$) patients compared to controls ($n=3$) (right). Other notations as in Figures 2 and 3.

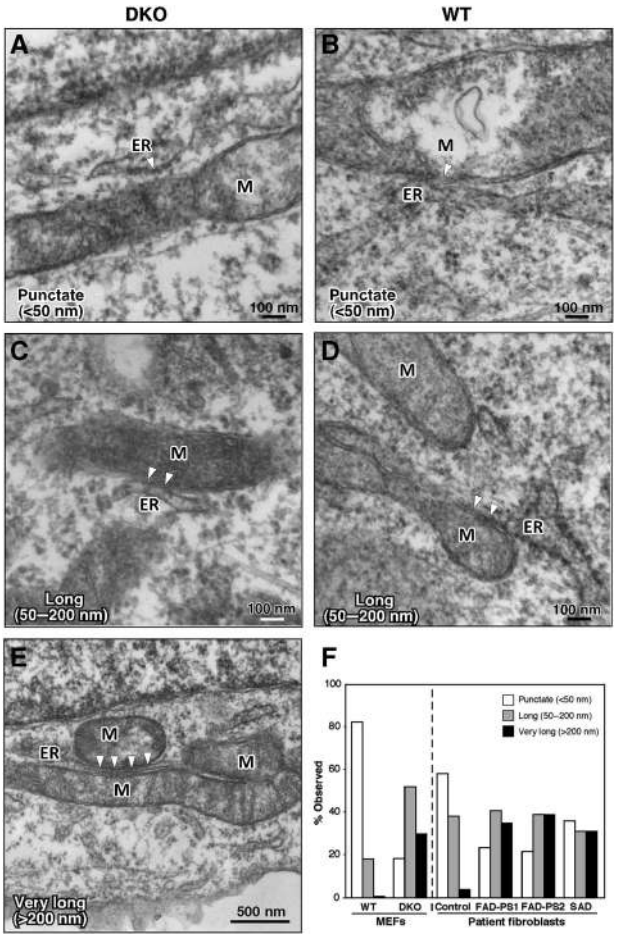

Figure 7 Electron microscopy of Ps-mutant and AD cells. (**A**, **C**, **E**) DKO MEFs. (**B**, **D**) WT MEFs. Note increased length of regions of contact between ER and mitochondria (M) (arrowheads) in DKO MEFs, and, in (**E**), a region of ER 'sandwiched' between two mitochondria. (**F**) Quantitation of ER–mitochondrial contact lengths in MEFs (~40 contacts analysed) and in fibroblasts from AD patients (~25 contacts). See also Supplementary Figure S8.

cells, as they were still highly enriched in the MAM compartment (Figure 8D). Thus, the deficiency in γ-secretase activity in Mfn2-KO cells supports the view that ER–mitochondrial communication is required for this functionality.

Given that mutations in presenilins increase both MAM function and ER–mitochondrial connectivity, whereas mutations in Mfn2 decrease the latter (de Brito and Scorrano, 2008), we asked if one could complement the other. Accordingly, we knocked down *Ps1* and *Ps2* transcripts simultaneously by ~80% in WT and Mfn2-KO MEFs (Supplementary Figure S9A), and measured phospholipid synthesis. We found that the decreased production of ^{3}H-PtdSer and ^{3}H-PtdEtn in Mfn2-KO MEFs was reversed when *Ps1/2* expression was knocked down (Figure 9A, left panel). Conversely, when we knocked down *Mfn2* transcripts in WT and Ps1/2-DKO MEFs by ~80% (Supplementary Figure S9B), we obtained the opposite result, as the increased phospholipid synthesis in the DKO MEFs was significantly reduced upon knocking down *Mfn2* expression (Figure 9A, right panel); notably, the phospholipid transport data correlated with the degree of ER–mitochondrial colocalization in these cells (Figure 9B). Analysis of the cells for duramycin sensitivity confirmed the biochemical findings, especially in the Ps1/2-DKO cells, where knockdown of *Mfn2* blunted the increase in Dura sensitivity relative to that in WT MEFs (Figure 9C). Finally, we measured CE synthesis (as assayed by LipidTox staining) and found that the increase in lipid droplet formation seen in Ps1/2-DKO MEFs was reversed by *Mfn2* silencing (Figure 9D).

Taken together, these results imply that presenilins and Mfn2 may affect the same pathway to regulate MAM activity and the apposition of ER to mitochondria.

Analysis of MAM function in cells deficient in γ-secretase activity

Our data clearly show that mutations in presenilins affect MAM function and ER–mitochondrial connectivity, but it was unclear whether the enzymatic activity of γ-secretase plays a direct role in these processes. Accordingly, we examined HeLa cells in which PS1 expression had been knocked

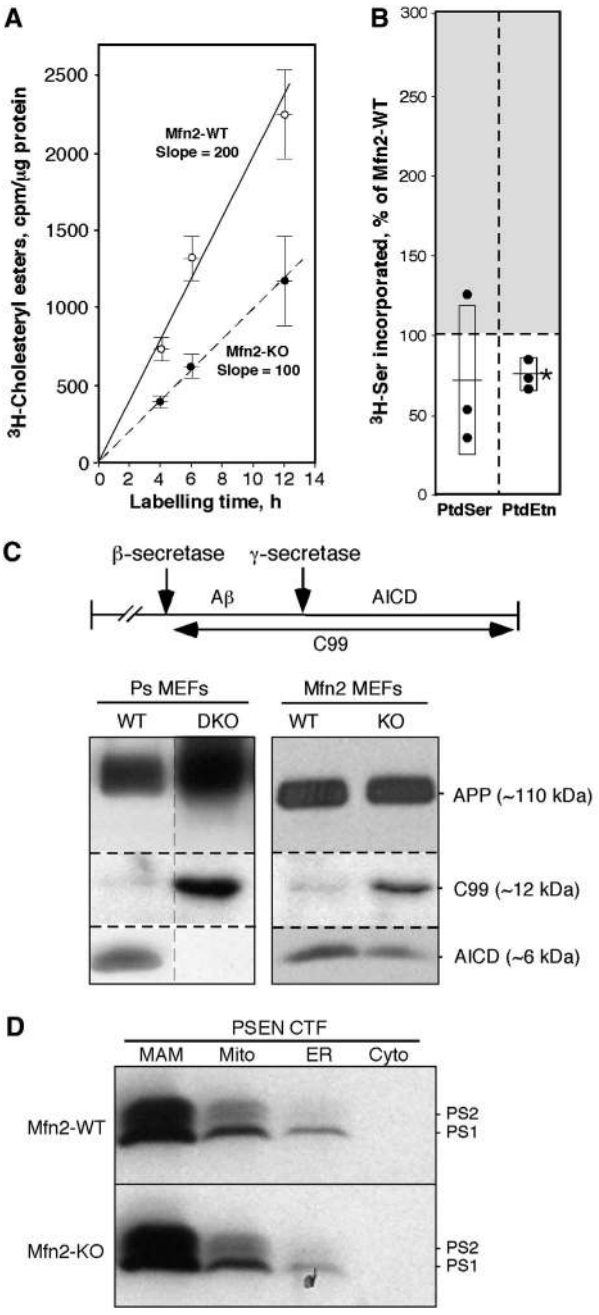

Figure 8 Analysis of MAM function in Mfn2-KO MEFs. (**A**) Kinetics of CE synthesis (performed as in Figure 2E) in Mfn2-KO MEFs (note decreased slope versus control). (**B**) Phospholipid synthesis after 6 h (as in Figure 4A) in Mfn2-KO cells (right) ($n = 3$). (**C**) Western blot to detect APP and its C-terminal cleavage products C99 and AICD (cleavage scheme at top) in Ps1/2-DKO and Mfn2-KO MEFs (image at the left is a composite of two non-adjacent lanes from the same gel; vertical dashed line indicates where the two lanes were apposed). Note the absence of AICD in DKO MEFs, and the shift in the ratio of C99:AICD in Mfn2-KO versus WT MEFs. (**D**) Subcellular distribution of presenilins in Mfn2-KO versus WT MEFs. Note that the loss of Mfn2 does not alter the predominant localization of presenilins in MAM. Other notations as in Figure 2.

down by shRNA (Supplementary Figure S9C) and asked if we could rescue MAM function by overexpressing either PS1-WT or a 'catalytically dead' construct encoding a D385A mutation in PS1 (Yu *et al*, 2000). Whereas adding back the WT version of PS1 rescued the knockdown phenotype, as expected, cells transfected with the D385A mutant showed an increase in ER–mitochondrial communication and MAM activity (as measured by phospholipid synthesis and lipid droplet formation; Supplementary Figure S10), similar to the increase observed in the PS1 knockdown MEFs (Figure 3C). The failure of 'catalytically dead' PS1 to rescue the knockdown phenotypes would suggest that γ-secretase activity itself is responsible for the regulation of MAM activity. However, it has been shown that full-length PS1 containing the D385A mutation cannot be cleaved into the N- and C-terminal fragments required for γ-secretase activity (Yu *et al*, 2000; Kim *et al*, 2005); this cleavage defect may also affect the proper subcellular localization of the protein (Chen *et al*, 2000). Moreover, PS1-D385A has been shown to depress the activity of WT PS1, in a dose-dependent manner (Kim *et al*, 2005), as well as to compete with WT PS1 for limiting factors required for γ-secretase activity (Thinakaran *et al*, 1997). For these reasons, we believe that overexpressing the D385A mutant basically mimics the KO/KD phenotype (Cheung *et al*, 2010), and therefore does not really answer the question as to whether γ-secretase activity itself regulates ER–mitochondrial communication and/or MAM function.

We therefore took a more direct biochemical approach. We treated various cell types with DAPT ((*N*-[*N*-(3,5-difluorophenacetyl)-L-alanyl]-S-phenylglycine t-butyl ester)), a highly specific γ-secretase inhibitor (Morohashi *et al*, 2006), for 24 h (Supplementary Figure S9D), and then assayed them for MAM function. DAPT had a profound effect on CE synthesis, as measured by the detection of lipid droplets, with an increase in the % of LipidTox-positive cells ranging from ~2-fold in MEFs to ~7-fold in 3T3 and HeLa cells (Figure 10A). Surprisingly, however, the increase in phospholipid transport was much lower (only on the order of ~20%; Figure 10B), a value far lower than the robust increases in phospholipid transport that were detected in cells (including MEFs) harbouring presenilin mutations (see Figure 4). We therefore quantitated the amount of ER–mitochondrial colocalization (performed as in Figure 6) in these DAPT-treated cells, and found that the drug had essentially no effect on the degree of ER–mitochondrial apposition (Figure 10C).

Taken together, these data imply that the catalytic activity of γ-secretase can have significant effects on MAM function (at least with respect to cholesterol ester synthesis) but appears to have little effect on establishing ER–mitochondrial connectivity. They also point to the possibility that there may be two separate classes of functions at the ER–mitochondrial interface: those required for 'horizontal' activity (i.e., intraorganellar enzymatic functions residing within the MAM compartment itself, as measured, for example, by CE synthesis) and those required to maintain 'vertical' MAM activity (i.e., interorganellar communication between ER and mitochondria, as measured, for example, by phospholipid transport).

Discussion

We previously showed that MAM is the predominant subcellular locus for presenilins and for γ-secretase activity (Area-Gomez *et al*, 2009). We now show that mutations in PS1, PS2, and APP can upregulate MAM function and increase ER–mitochondrial connectivity significantly, implying that presenilins are negative regulators of these beha-

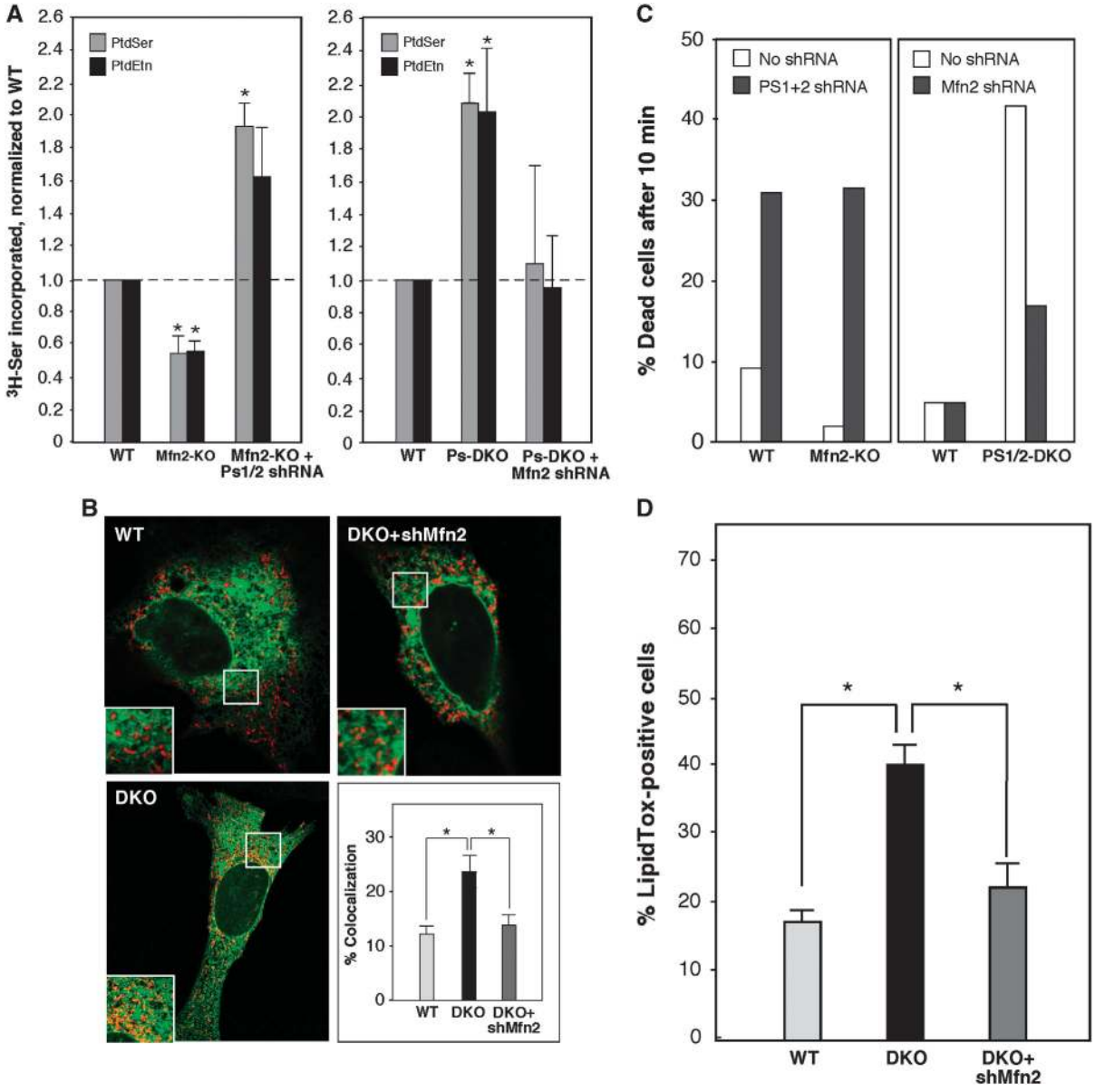

Figure 9 Rescue of phospholipid (PL) synthesis in Ps- and Mfn2-mutant MEFs. (**A**) Synthesis of ^{3}H-PtdSer and ^{3}H-PtdEtn after labelling for 6 h with ^{3}H-Ser in the indicated MEFs. Left: Note that PL synthesis was *decreased* in Mfn2-KO MEFs compared to WT but was restored upon knockdown of *Ps1*+*Ps2* (average of four experiments ± s.e.). A control knockdown of *Ps1*+*Ps2* in WT MEFs increased PL synthesis, as expected (not shown). Right: In the converse experiment, note that PL synthesis was *increased* in Ps1 + Ps2 DKO MEFs compared to WT but was restored upon knockdown of *Mfn2* (average of five experiments ± s.e.). A control knockdown of *Mfn2* in WT MEFs reduced PL synthesis, as expected (not shown). (**B**) Examples (as in Figure 6A), and quantitation (average of 20 cells analysed ± s.e.), of ER–mitochondrial contacts in WT, Ps1 + Ps2-DKO, and DKO cells 'rescued' by knockdown of *Mfn2*. (**C**) Effect of presenilins and Mfn2 on duramycin sensitivity. Note that Dura sensitivity correlates with the change in PtdEtn synthesis shown in (**A**). (**D**) Quantitation of lipid droplets in *Ps1*+*Ps2* DKO MEFs upon knockdown of *Mfn2* (average of five images ± s.e.). Other notation as in Figure 2.

viours. Moreover, we found that cells from patients with SAD, in which PS1, PS2, and APP structure (but perhaps not expression; McMillan *et al*, 2000; Sato *et al*, 2001) are normal, also display the same hallmarks of upregulated MAM function and ER–mitochondrial communication as do those with FAD.

Because MAM dysfunction is the common denominator underlying the phenotypes seen in both FAD and SAD, we therefore propose that increased MAM activity and ER–mitochondrial communication lies at the heart of AD pathogenesis (Figure 11). In support of this view, we note that many of the biochemical and morphological phenotypes associated with AD—altered cholesterol, phospholipid, glucose, and calcium metabolism, aberrant mitochondrial behaviour and function, and notably, altered Aβ production—are the very functions that are associated with MAM and with connections between ER and mitochondria.

The first clue that MAM might be involved in AD came from the observation that presenilins and γ-secretase activity are enriched in MAM (Area-Gomez *et al*, 2009). This speculation was reinforced by the finding that MAM is an LR-like domain (Figure 1; Hayashi and Fujimoto, 2010; Williamson *et al*, 2011; Fujimoto *et al*, 2012), which is consistent with previous

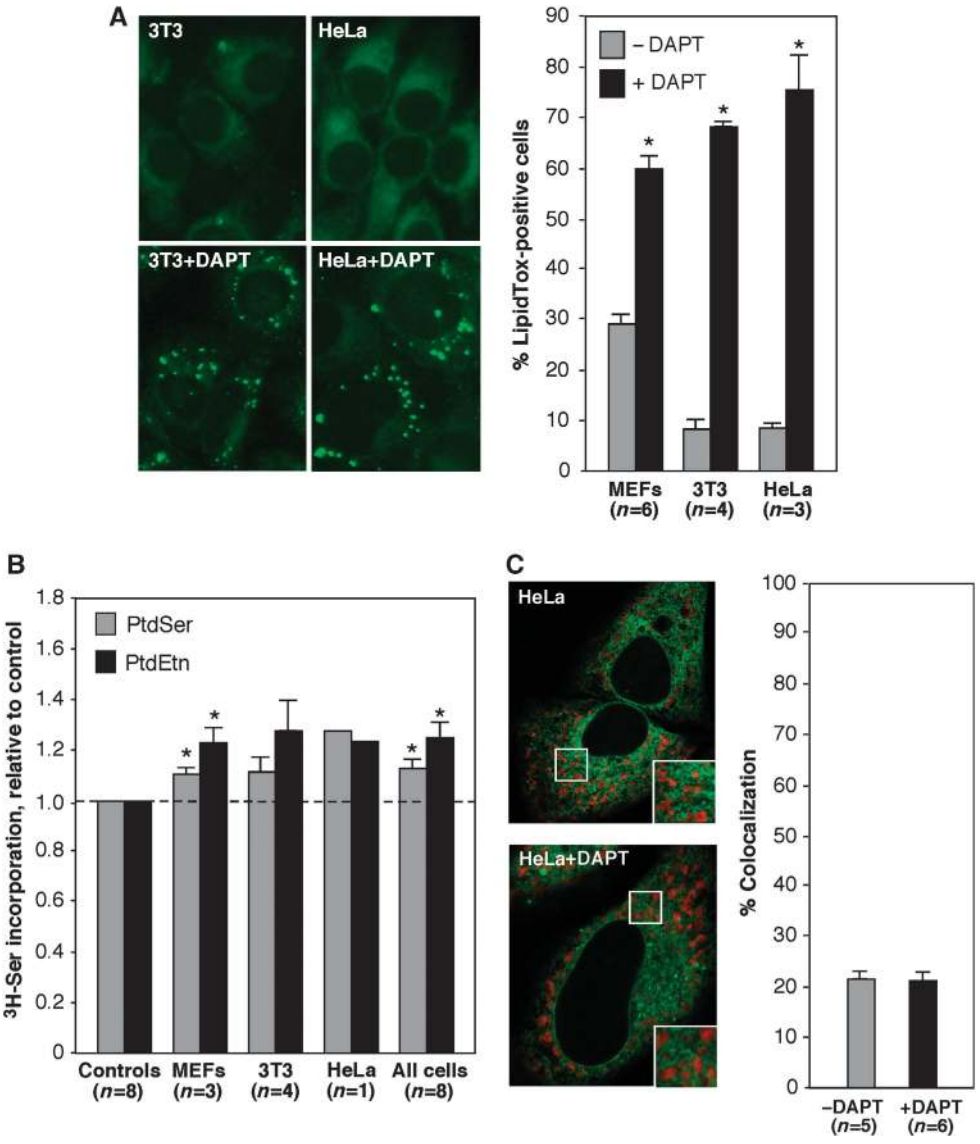

Figure 10 MAM function in cells deficient in γ-secretase activity. (**A**) Detection of lipid droplets in HeLa and 3T3 cells treated with 5 μM DAPT for 24 h. Examples of LipidTox staining (left) and quantitation (right; n = number of images analysed, with a total of ~500 cells analysed ± s.e.), as in Figure 3. Note the large increase in LipidTox staining, ranging from ~200 to ~700% over control. (**B**) Phospholipid transport in the indicated cells (as in Figure 4). Note the modest increase in PtdSer and PtdEtn synthesis, of only ~20%. (**C**) Colocalization of ER and mitochondria (as in Figure 6) in HeLa cells. Note that DAPT had no effect on the degree of colocalization. Other notation as in Figure 2.

data showing that APP processing to produce Aβ depends on LRs (Ehehalt *et al*, 2003; Urano *et al*, 2005; Vetrivel *et al*, 2005; Kosicek *et al*, 2010; Nesic *et al*, 2012). Apart from the lack of appropriate markers to detect MAM, one of the reasons that MAM was overlooked as a detergent-resistant membrane, and as the region in which PS's, APP, and γ-secretase activity are enriched, may be that most methods used to isolate rafts do not separate the PM from intracellular membranes (Macdonald and Pike, 2005). Thus, intracellular DRMs like MAM will be co-isolated with PM rafts during the subfractionation process, obscuring the localization of PS's and γ-secretase activity at ER–mitochondria connections. This ambiguity might help explain earlier observations indicating that, along with the presenilins, the other components of the γ-secretase complex—nicastrin, APH-1, and PEN-2—are not only present in the MAM (Area-Gomez *et al*, 2009) but are also enriched in DRMs (Vetrivel *et al*, 2005).

Furthermore, the fact that MAM is a DRM may also help explain the lack of consensus regarding the subcellular localization of presenilins and γ-secretase activity, as detecting proteins embedded in DRMs can be technically challenging (Schon and Area-Gomez, 2010). It may also explain why MAM markers such as VDAC (Szabadkai *et al*, 2006) and calnexin (Myhill *et al*, 2008) were found in some studies of PM rafts (Foster *et al*, 2003; Zheng *et al*, 2009) and why Aβ was reported to be present in mitochondria (Lustbader *et al*, 2004; Manczak *et al*, 2006). Likewise, crude mitochondrial preparations contain MAM that can lead one into thinking that mitochondria contain *bona fide* LRs (Sorice *et al*, 2009) when in fact they do not (Zheng *et al*, 2009). It has long been known that presenilins, APP, Aβ, and γ-secretase activity are enriched in LRs/DRMs (Urano *et al*, 2005; Kosicek *et al*, 2010), but it had always been assumed that these rafts were located at the PM (Lajoie and Nabi, 2010). Our data are consistent

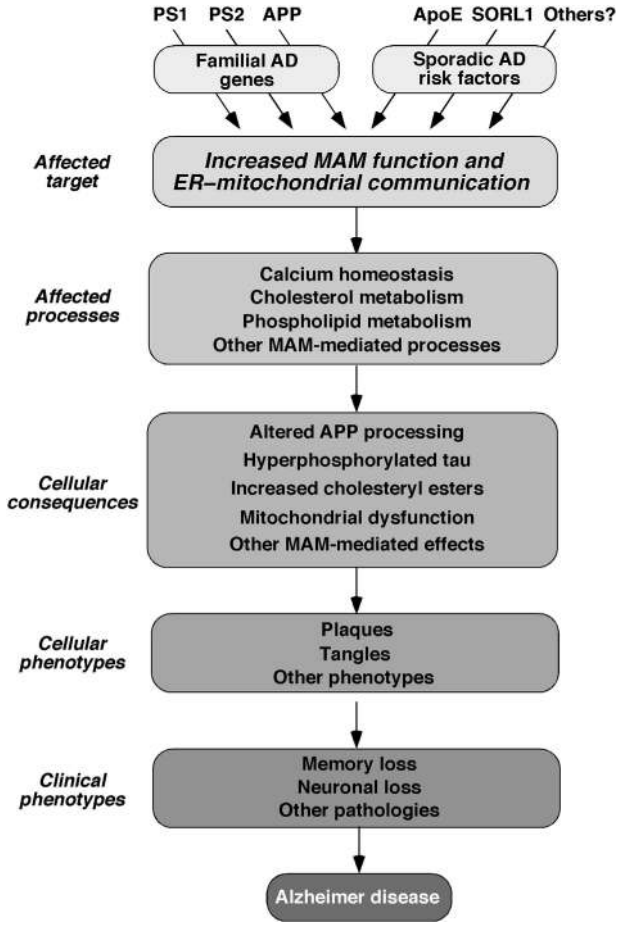

Figure 11 A model of pathogenesis of Alzheimer disease. In broad view, underlying genotypes that either cause AD directly (in the case of FAD) or are risk factors that predispose to developing AD (in the case of SAD) increase MAM function and/or ER–mitochondrial communication. This increase affects various MAM-mediated processes (either positively or negatively, depending on the particular gene/function involved), which in turn give rise to the various phenotypes seen in AD. See text for details.

with an alternate interpretation, namely, that APP processing to produce Aβ occurs not at LRs in the PM, but intracellularly in the MAM (Hayashi and Fujimoto, 2010). We note that several groups have suggested the existence of intracellular rafts in the ER or mitochondria (Browman *et al*, 2006); we believe that these LRs/DRMs are, in fact, MAMs (Hayashi and Fujimoto, 2010; Williamson *et al*, 2011; Fujimoto *et al*, 2012).

As a locus for the integration of key cellular functions and signalling (Hayashi *et al*, 2009), MAM apparently requires a more rigid liquid-ordered phase to recruit, orient, regulate, and limit the lateral mobility of the membrane proteins within its boundaries, so as to promote the cross-talk of mitochondria and ER. If MAM is indeed an LR, then alterations in its structure and composition may affect profoundly the cellular functions localized within it. It is possible that the loss or alteration of γ-secretase activity (via, e.g., mutations in presenilins and APP in the case of FAD) affects the structure and lipid composition of cellular membranes in general and of MAM in particular, especially in AD (Chan *et al*, 2011). Conversely, alterations in MAM via, for example, disrupting Mfn2 expression, can also affect γ-secretase activity, with the physical distance separating ER from mitochondria playing a critical role in the regulation of MAM function (Csordas *et al*, 2010). Thus, we believe that perturbations in ER–mitochondrial connectivity are the key element underlying AD pathogenesis, and perhaps other neurodegenerative diseases as well (Schon and Przedborski, 2011).

As noted above, many of the apparently unrelated cellular functions that are misregulated in AD can be ascribed to increased MAM function and ER–mitochondrial connectivity. First, it has long been known that AD patients have elevated ACAT levels (Pani *et al*, 2009a), elevated cholesterol and/or CEs (Stefani and Liguri, 2009; Pani *et al*, 2009a), and deposition of lipid droplets in peripheral cells (Pani *et al*, 2009b; Mandas *et al*, 2012) and in neurons (Gómez-Ramos and Asunción Morán, 2007). In addition, there is compelling evidence that MAM plays a role in lipid droplet formation (Walther and Farese, 2009) and that both PtdEtn synthesis (Nesic *et al*, 2012) and ACAT activity (Puglielli *et al*, 2001, 2004) are required for Aβ production. The connection of MAM-localized ACAT1 to AD is intriguing: the enzyme is absolutely required for the generation of Aβ, by modulating the equilibrium between free and esterified cholesterol (Puglielli *et al*, 2001, 2003, 2004; Pottekat and Menon, 2004), presumably as a result of its affects on APP processing (Huttunen *et al*, 2009a, b; Bryleva *et al*, 2010). While it is unclear how mutated presenilins affect Aβ production, it has been shown that pathogenic mutations in PS1 affect the conformation of the γ-secretase active site (Chau *et al*, 2012). Thus, one possibility is that altered cholesterol and lipid composition within the MAM membrane changes the orientation of APP and its cleavage by γ-secretase, and hence, the generation of total Aβ and an alteration in the ratio of $A\beta_{42}$:$A\beta_{40}$ (Uemura *et al*, 2011; Holmes *et al*, 2012). In support of this view, we note that the membrane thickness of LRs is greater than that of the surrounding bilayer (Risselada and Marrink, 2008; Lingwood and Simons, 2010), and that the thickness of model membranes affects the cleavage specificity of γ-secretase as well as the relative amounts of $A\beta_{40}$ and $A\beta_{42}$ (Winkler *et al*, 2012). A connection between MAM and Aβ production is also supported by the recent finding that extracellular plaques have an intracellular origin, and that this process is mediated by sphingomyelin and GM1 gangliosides (Yuyama and Yanagisawa, 2010), both of which are components of MAM and which play a significant role in its regulation (Sano *et al*, 2009; Grimm *et al*, 2011, 2012). In addition, the finding of increased phospholipid synthesis in PS-mutant cells, indicative of increased cross-talk between ER and mitochondria (Voelker, 2005), is consistent with the reported aberrations in phospholipid profiles in AD patients (Pettegrew *et al*, 2001; Chan *et al*, 2011).

Alterations in MAM likely affect other cellular functions as well. One of the most critical of these is calcium homeostasis (Csordas *et al*, 2010; Giacomello *et al*, 2010), as MAM is highly enriched in the sarco-ER calcium-ATPase (de Meis *et al*, 2010), the sigma-1 receptor (Hayashi and Fujimoto, 2010), ryanodine receptors (RyRs) (García-Pérez *et al*, 2008), and inositol-1,4,5-trisphosphate receptors (IP3Rs) (Hayashi *et al*, 2009). Thus, increased ER–mitochondrial communication in AD could explain the altered intracellular Ca^{2+} trafficking via RyRs (Stutzmann *et al*, 2006) and IP3Rs (Leissring *et al*, 1999; Zampese *et al*, 2011), leading to the

aberrant calcium homeostasis found in AD patients (Bezprozvanny and Mattson, 2008). Surprisingly, Zampese *et al* (2011) concluded that PS2, but not PS1, modulates ER–mitochondria interactions and calcium cross-talk, a finding that differs with the data reported here showing that *both* presenilin isoforms mediate MAM function and ER–mitochondrial communication; it also differs with the observation that mutations in PS1 enhance IP3R-mediated calcium trafficking (Cheung *et al*, 2008, 2010; Mattson, 2010), which is clearly an MAM-mediated function (Hayashi *et al*, 2009). Their findings would also be difficult to reconcile with the fact that mutations in PS1 are more prevalent in FAD than are those in PS2, and result in a more 'severe' clinical course (Jayadev *et al*, 2010), and would also imply that the mechanisms by which these two highly related proteins cause FAD are radically different, even though both proteins are components of the γ-secretase complex. However, we note that Zampese *et al* (2011) relied on experiments in which the presenilin and multiple reporter constructs were overexpressed transiently, which may have introduced a degree of ambiguity in the interpretation of their data (Stieren *et al*, 2010). In addition, these transfections were performed in cells expressing endogenous WT chromosomal PS1 and PS2 alleles, which could have resulted in potential feedback of the introduced constructs on their regulation, a potential problem that was circumvented in our experimental design, which relied instead on knockdown and knockout constructs and on AD patient cells expressing endogenous mutated alleles. We also note that, contrary to what we observed here, Zampese *et al* (2011) found reductions in *Mfn2* expression upon knockdown of the presenilins; such reductions may have inadvertently masked any effect on MAM function due to reduced presenilin expression. Taken together, we believe that the conclusion of Zampese *et al* (2011) that only PS2, and not PS1, affects MAM behaviour is open to question.

Mitochondrial dysfunction in AD has been reported extensively (Su *et al*, 2010), but there is no clear evidence as to whether it is cause or effect. Altered connections between ER and mitochondria would almost certainly affect mitochondrial dynamics (e.g., shape, distribution, and movement; Kornmann *et al*, 2011) and function (e.g., oxidative energy metabolism, calcium buffering capacity, and free radical production; Peterson and Goldman, 1986; Hirai *et al*, 2001; Gibson and Huang, 2004; Bubber *et al*, 2005), and thus may be the underlying cause of the reported aberrant mitochondrial phenotypes seen in AD (Su *et al*, 2010).

Our assays of MAM function upon inhibition of γ-secretase activity yielded the surprising result that whereas the catalytic activity of the enzyme is required for at least some aspects of MAM function, it is apparently not required to maintain ER–mitochondrial connectivity. Together with the Mfn2 rescue experiments, this result, which was obtained in cells expressing endogenous WT presenilins, implies that the presenilin protein itself (and not just its proteolytic activity) is acting as a regulator of the distance between ER and mitochondria (Csordas *et al*, 2010). A corollary of this finding is that the presenilins might play a role in ER–mitochondrial communication independent of their enzymatic function. These results also underscore the fact that MAM function and ER–mitochondrial communication are two separate aspects of this single cellular subdomain: on the one hand, MAM is a true compartment of the ER, with its own suite of biochemical activities, whereas on the other, it is a bridge that connects two organelles, namely the ER and the mitochondria. We note, however, that all of our data indicate that in AD, both aspects—MAM function and interorganellar distance—are affected, but whether both aspects must be affected consistently in order to cause disease remains to be determined.

Finally, our findings have implications for understanding the genetics of AD (Hollingworth *et al*, 2011; Naj *et al*, 2011). Most presenilin mutations causing FAD are dominant and are presumed to cause a gain of function (De Strooper *et al*, 1998; Cheung *et al*, 2010). However, the increased MAM function in PS-KD and -KO cells reported here imply that the effects of many (but probably not all; Chavez-Gutierrez *et al*, 2012) pathogenic PS1 mutations are more likely to be due to loss of function or to a gain of negative function (McMillan *et al*, 2000; Bentahir *et al*, 2006; Shen and Kelleher, 2007; Heilig *et al*, 2010; Jayadev *et al*, 2010; Cacquevel *et al*, 2012).

We believe that the increased MAM function and ER–mitochondrial cross-talk found in all PS mutant cells analysed could help explain some of the features and early events in AD, such as elevated serum cholesterol levels, mitochondrial dysfunction, oxidative stress, and calcium deregulation (Schon and Area-Gomez, 2010), which are all upstream of the appearance of plaques and tangles (Pratico and Delanty, 2000) and which are detected routinely in AD patients. As such, upregulated MAM function could play a hitherto unrecognized and critical role in the pathogenesis of AD (Schon and Area-Gomez, 2010) that may help us to understand better this devastating disease.

Materials and methods

Cells and reagents

WT, Ps1-KO, Ps2-KO, and DKO mouse MEFs were gifts of Dr Bart De Strooper (University of Leuven). WT and Mfn2-KO MEFs were gifts of David Chan (California Institute of Technology). PS1- and APP-mutant FAD cells were kind gifts of Gary E Gibson (Cornell University) and Richard Cowburn (Karolinska Institute). Other AD and control cell lines were obtained from the Coriell Institute for Medical Research (Camden, NJ) (see Supplementary Table S1). We used antibodies to PS1 (aa 1–65 (Calbiochem 529591) and aa 303–316 (Calbiochem PC267)), PEMT (a gift of Joan Vance, University of Alberta), VDAC1 (Abcam ab15895), ACAT1 (Abcam ab39327), Na^+/K^+-ATPase (Abcam ab7671), SRC tyrosine kinase (Abcam ab32102), NDUFA9 (monoclonal; Molecular Probes A21344), MFN2 (Abcam ab50838), and SSRα (a gift of Howard Worman and Martin Wiedemann, Columbia University). Thin layer chromatography (TLC) silica plates were from EMD Biosciences (5748-7). Phosphatidylserine (P7769), phosphatidylethanolamine (60648), cholesteryl palmitate (C6072), cholesteryl oleate (C9253), lipid markers for TLC (P3817), cinnamycin (C5241), duramycin (D3168), and DAPT (D5942) were from Sigma. Radiolabelled ^{3}H-serine and ^{3}H-cholesterol were from Perkin-Elmer; ^{3}H-oleoyl-CoA was from Moravek Biochemicals (MT1649); and fatty acid-free bovine serum albumin (FAF-BSA) was from MP Biomedical (820472).

Subcellular fractionation and western blotting

Purification of ER, MAM, and mitochondria was performed and analysed as described (Area-Gomez *et al*, 2009).

Isolation of LRs

To identify detergent-resistant domains, samples were resuspended in 400 μl of isolation buffer (IB: 250 mM mannitol, 5 mM HEPES pH 7.4, and 0.5 mM EGTA) containing 1% Triton X-100 and incubated at 4°C with rotation for 1 h. Samples were adjusted to 80% sucrose,

placed at the bottom of a 5–30% sucrose gradient, and centrifuged at 250 000 *g* for 18 h. After fractionation, equal volumes of each fraction were loaded on an SDS–PAGE gel and analysed by western blot.

Measurement of cholesterol species

Quantification of total cholesterol and CEs was performed using the Cholesterol/Cholesteryl Ester Quantitation kit from Calbiochem (428901).

Lipid droplet staining

Staining of lipid droplets was performed using HCS LipidTox™ Deep Green neutral lipid stain (Invitrogen H34475) according to manufacturer's instructions. Lipid droplet staining was quantified using ImageJ. When reported as intensities, the values in the text represent the product of the intensity and the area covered by the fluorescent signal above background in every cell examined. For each cell type and/or condition, we took between 15 and 20 images for analysis. The images were first taken at lower magnification ($\times 20$) in order to view 50–100 cells per field. The numbers reported in the text represent the averages derived from the quantification of staining in 500–600 cells.

For lipid droplet staining by Oil Red O, we first prepared a stock solution (35% Oil Red O in isopropanol), stirring the mix for 12 h and filtering it before use. Cultured cells were fixed in 10% formalin in PBS for at least 1 h and washed twice in ddH_2O. The plates were incubated in 60% isopropanol for 5 min at RT, the alcohol was discarded, and the cells were allowed to dry completely at RT. One microlitre of a filtered Oil Red O working solution (60% stock solution in H_2O) was added to the cells at RT for 10 min. The Oil Red O solution was removed and the samples were immediately washed in ddH_2O before acquiring images under the microscope.

Analysis of phospholipid synthesis in cultured cells

Cells were incubated for 2 h with serum-free medium to ensure removal of exogenous lipids. The medium was then replaced with MEM containing 2.5 μCi/ml of ^{3}H-serine for the indicated periods of time. The cells were washed and collected in DPBS, pelleted at 2500 *g* for 5 min at 4°C, and resuspended in 0.5 ml water, removing a small aliquot for protein quantification. Lipid extraction was done by the Folch method. Briefly, three volumes of chloroform/methanol 2:1 were added to the samples and vortexed. After centrifugation at 8000 *g* for 5 min, the organic phase was washed twice with two volumes of methanol/water 1:1, and the organic phase was blown to dryness under nitrogen. Dried lipids were resuspended in 60 μl of chloroform/methanol 2:1 and applied to a TLC plate. Phospholipids were separated using two solvents, composed of petroleum ether/diethyl ether/acetic acid 84:15:1 v/v and chloroform/methanol/acetic acid/water 60:50:1:4 v/v. Development was performed by exposure of the plate to iodine vapour. The spots corresponding to the relevant phospholipids (identified using co-migrating standards) were scraped and counted in a scintillation counter (Packard Tri-Carb 2900TR).

Analysis of phospholipid synthesis in subcellular fractions

Crude mitochondrial fractions were isolated from MEFs as described (Area-Gomez *et al*, 2009). Two hundred micrograms were incubated in a final volume of 200 μl of phospholipid synthesis buffer (10 mM $CaCl_2$, 25 mM HEPES pH 7.4, and 3 μCi/ml ^{3}H-Ser) for 30 min at 37°C. The reaction was stopped by addition of three volumes of chloroform/methanol 2:1. Lipid extraction and TLC analysis were performed as described above.

Assay of ACAT activity

To measure ACAT activity *in vivo*, whole cells were incubated in serum-free medium for 2 h to remove all exogenous lipids. After that, 2.5 μCi/ml of ^{3}H-cholesterol was added to FBS-free DMEM containing 2% FAF-BSA, allowed to equilibrate for at least 30 min at 37°C, and the radiolabelled medium was added to the cells for the indicated periods of time. Cells were then washed and collected in DPBS, removing a small aliquot for protein quantification. Lipids were extracted as described above and samples were analysed by TLC along with an unlabelled CE standard. A mixture of chloroform/methanol/acetic acid 190:9:1 was used as solvent. Iodine stains corresponding to CE bands were scraped and counted.

Cinnamycin and duramycin assays

Cinnamycin and duramycin were diluted in FBS-free DMEM to the appropriate concentration and added to the cells for the indicated time periods at 37°C. After incubation, cells were washed in PBS twice before testing cell viability by Live/Dead assay (Invitrogen #L3224) according to manufacturer's instructions. Samples were then analysed under the microscope and cell death was quantified by counting live (green) and dead (red) cells manually. To detect fluorescent cinnamycin with FL-SA-Ro, cells were washed three times with Hanks' buffered saline containing 0.5% BSA (0.5% BSA–HBS) and incubated with 50 μg/ml Cy3-conjugated cinnamycin (FL-SA-Ro) for 30 min at 37°C. Cells were then washed with 0.5% BSA–HBS and analysed under the microscope. To visualize cell morphology, cells were then counterstained with 5 mM calcein (AnaSpec #89203) in PBS for 20 min at room temperature, fixed in 4% paraformaldehyde, mounted, and analysed under the microscope.

Analysis of ER–mitochondrial apposition

Cells under were co-transfected with GFP-Sec61-β (Addgene plasmid #15108) and DsRed-Mito (Clontech, #632421) at a 1:1 ratio, using Lipofectamine 2000 (Invitrogen, #11668-027) in serum-free DMEM. Twelve hours post transfection, cells were analysed in a single-plane with a Zeiss LSM510 microscope. Interactions between mitochondria and ER were calculated using Image J software (http://rsbweb.nih.gov/ij/), determining the area occupied by one organelle and using its signal as a mask for the other one. The various 'colocalization' data sets were compared using Mander's coefficient.

Transmission EM

Cells were fixed with 2.5% glutaraldehyde in 0.1 M Sorenson's phosphate buffer (pH 7.2) for at least 1 h. Cells were then postfixed for 1 h with 1% OsO_4 in Sorenson's buffer. Staining was performed using 1% tannic acid. After dehydration, cells were embedded in a mixture of Lx-112 (Ladd Research Industries) and Embed-812 (EMS, Fort Washington, PA). Thin sections, cut on an MT-7000 ultramicrotome, were stained with uranyl acetate and lead citrate, and examined in a JEOL JEM-1200 EXII electron microscope. Pictures were taken on an ORCA-HR digital camera (Hamamatsu) and recorded with an AMT Image Capture Engine.

Transcriptional silencing

To knockdown mouse *Ps1*, small hairpin (sh) RNA oligonucleotide M2 @ nt 179–197 in mouse *Psen1* (Genbank NM_008943: gac aggtggtggaacaaga) and mismatch control shRNA M3 (gacagg**a**gg**a**g gaacaaga; mismatches in bold) were inserted into pSUPER-Retro-Puro vector pSR (OligoEngine). We also replaced the puromycin-resistance cassette with a blasticidine-resistance cassette inserted at the *Nhe*I-*Dra*III sites in the vector, generating pSR-Blast, to allow for 'double transduction' using two different selection markers to increase shRNA expression. Viral supernatants (3 ml) from plasmid-transfected Amphotrophic Phoenix ΦNX-A packaging cells supplemented with polybrene were added to immortalized mouse MEFs (derived from primary MEFs of mixed C57Bl/6-129 mice, using a 3T3 subculture schedule; Todaro and Green, 1963), seeded 1 day prior to infection at 100 000/well in 6-well culture plates, followed by infection for 24 h. Cells were selected in medium containing puromycin, blasticidine, or both antibiotics, for 14 days. Using this protocol, PS1 expression was reduced by >75% (Supplementary Figure S3). For complementation experiments, human WT PS1 and mutated PS1 (A246E) cloned in pSuper-Retro-Neo and viral supernatants were prepared as described above. Transduced cells were selected using G418.

To knockdown presenilin expression, shRNAs against mouse *Psen1* (Sigma SASI_Mm01_00048853) and *Psen2* (Sigma SASI_Mm02_00310708) and against human *PSEN1* (Sigma SASI_Hs01_00043630) and *PSEN2* (Sigma SASI_Hs01_00033516) were transfected transiently together into relevant mouse and human cells, respectively, according to manufacturer's recommendations. Briefly, cells plated at low confluence were transfected with each shRNA to a final concentration of 30 nM, using Lipofectamine 2000 (Invitrogen, 11668-027) at a 1:1 ratio in serum-free DMEM. After 5 h, the medium was changed to 2% FBS DMEM and the cells were incubated for 12 more hours. Successful silencing of the targeted proteins was checked by western blot. To knockdown mouse *Mfn2* in WT and Ps1/2-DKO MEFs, shRNA against *Mfn2*

(Sigma SASI_Mm01_00027313) was transfected and analysed in a similar fashion.

Where indicated, cells were transfected with pcDNA3-PS1WT or pcDNA3-PS1D385A mutant (a kind gift of Dr Tae-Wan Kim, Columbia University) at a 1:1 ratio, using Lipofectamine 2000 (Invitrogen #11668-027) in serum-free DMEM. After 5 h, the medium was changed to DMEM containing 2% FBS. Cells were analysed 12 h post transfection.

Inhibition of γ-secretase activity

Cells were treated with 2–5 μM DAPT in 2% FBS DMEM, a highly specific γ-secretase inhibitor (Morohashi *et al*, 2006), for 24 h. Following treatment, the cells were collected in PBS and then analysed, as described.

Quantitative RT–PCR (qRT–PCR)

Total RNA was extracted from MEFs using TRIzol® Reagent (Invitrogen 15596-018) according to manufacturer's instructions, and was quantified by NanoDrop2000 (Thermo Scientific). One microgram of total RNA was used to obtain cDNA by RT–PCR using a High Capacity cDNA Reverse Transcription Kit (Applied Biosystems; PN 4368813, 4374966). Real-time PCR was performed in triplicate in a StepOnePlus™ Real-Time PCR System (Applied Biosystems; 4376600). The expression of each gene under study was analysed using specific predesigned TaqMan Probes and normalizing against *Gapdh* expression (Applied Biosystems, 4352339E) as an internal standard.

Supplementary data

Supplementary data are available at *The EMBO Journal* Online (http://www.embojournal.org).

Acknowledgements

We thank Kristy Brown for assistance with the electron microscopy; Bart de Strooper for providing the Ps-mutant MEFs; David Chan for providing the Mfn2-mutant MEFS; Mariska te Lindert and Bé Wieringa for assisting in establishing the Ps1-KD MEFs; Tae-Wan Kim for providing PS1 constructs; Karen Duff, Ellen Steinbart, Gary Gibson, and Richard Cowburn for providing patient cells; and Salvatore DiMauro, Robert W Gilkerson, Michio Hirano, Larry Honig, and Serge Przedborski for comments. This work was supported by grants from the Ara Parseghian Medical Research Foundation (to SLS), the Ministry of Education, Culture, Sports, Science, and Technology of Japan (to MU and JI), the Japan Science and Technology Agency (to JI), the National Institute of Aging (AG005136) and Veterans Affairs Research Funds (to TDB), the John Douglas French Alzheimer Foundation (to EAG), and the American Health Assistance Foundation, the Ellison Medical Foundation, the Alzheimer Drug Discovery Foundation, the US Department of Defense (W911NF-12-1-0159), and the Marriott Mitochondrial Disorder Clinical Research Fund (to EAS).

Author contributions: EA-G conceived and designed experiments; acquired, analysed, and interpreted data; wrote the paper. MCLC, MDT, CG-L, AJCG, and MM acquired, analysed, and interpreted data. JI, MU, and TDB provided critical reagents and helped acquire data. SLS provided critical experimental expertise and technology and helped acquire data. EAS conceived and designed experiments; analysed and interpreted data; wrote the paper.

Conflict of interest

The authors declare that they have no conflict of interest.

References

Ankarcrona M, Hultenby K (2002) Presenilin-1 is located in rat mitochondria. *Biochem Biophys Res Commun* **295:** 766–770

Annaert WG, Levesque L, Craessaerts K, Dierinck I, Snellings G, Westaway D, St George-Hyslop P, Cordell B, Fraser P, De Strooper B (1999) Presenilin 1 controls γ-secretase processing of amyloid precursor protein in pre-golgi compartments of hippocampal neurons. *J Cell Biol* **147:** 277–294

Area-Gomez E, de Groof AJ, Boldogh I, Bird TD, Gibson GE, Koehler CM, Yu WH, Duff KE, Yaffe MP, Pon LA, Schon EA (2009) Presenilins are enriched in endoplasmic reticulum membranes associated with mitochondria. *Am J Pathol* **175:** 1810–1816

Bentahir M, Nyabi O, Verhamme J, Tolia A, Horre K, Wiltfang J, Esselmann H, De Strooper B (2006) Presenilin clinical mutations can affect γ-secretase activity by different mechanisms. *J Neurochem* **96:** 732–742

Bezprozvanny I, Mattson MP (2008) Neuronal calcium mishandling and the pathogenesis of Alzheimer's disease. *Trends Neurosci* **31:** 454–463

Browman DT, Resek ME, Zajchowski LD, Robbins SM (2006) Erlin-1 and erlin-2 are novel members of the prohibitin family of proteins that define lipid-raft-like domains of the ER. *J Cell Sci* **119:** 3149–3160

Bryleva EY, Rogers MA, Chang CC, Buen F, Harris BT, Rousselet E, Seidah NG, Oddo S, LaFerla FM, Spencer TA, Hickey WF, Chang TY (2010) ACAT1 gene ablation increases 24(S)-hydroxycholesterol content in the brain and ameliorates amyloid pathology in mice with AD. *Proc Natl Acad Sci USA* **107:** 3081–3086

Bubber P, Haroutunian V, Fisch G, Blass JP, Gibson GE (2005) Mitochondrial abnormalities in Alzheimer brain: mechanistic implications. *Ann Neurol* **57:** 695–703

Cacquevel M, Aeschbach L, Houacine J, Fraering PC (2012) Alzheimer's disease-linked mutations in presenilin-1 result in a drastic loss of activity in purified γ-secretase complexes. *PLoS ONE* **7:** e35133

Chan RB, Oliveira TG, Cortes EP, Honig LS, Duff KE, Small SA, Wenk MR, Shui G, Di Paolo G (2011) Comparative lipidomic analysis of mouse and human brain with Alzheimer's disease. *J Biol Chem* **287:** 2678–2688

Chau DM, Crump CJ, Villa JC, Scheinberg DA, Li YM (2012) Familial Alzheimer disease presenilin-1 mutations alter the active site conformation of γ-secretase. *J Biol Chem* **287:** 17288–17296

Chavez-Gutierrez L, Bammens L, Benilova I, Vandersteen A, Benurwar M, Borgers M, Lismont S, Zhou L, Van Cleynenbreugel S, Esselmann H, Wiltfang J, Serneels L, Karran E, Gijsen H, Schymkowitz J, Rousseau F, Broersen K, De Strooper B (2012) The mechanism of γ-secretase dysfunction in familial Alzheimer disease. *EMBO J* **31:** 2261–2274

Chen F, Yang DS, Petanceska S, Yang A, Tandon A, Yu G, Rozmahel R, Ghiso J, Nishimura M, Zhang DM, Kawarai T, Levesque G, Mills J, Levesque L, Song YQ, Rogaeva E, Westaway D, Mount H, Gandy S, St George-Hyslop P *et al* (2000) Carboxyl-terminal fragments of Alzheimer β-amyloid precursor protein accumulate in restricted and unpredicted intracellular compartments in presenilin 1-deficient cells. *J Biol Chem* **275:** 36794–36802

Cheung KH, Mei L, Mak DO, Hayashi I, Iwatsubo T, Kang DE, Foskett JK (2010) Gain-of-function enhancement of IP_3 receptor modal gating by familial Alzheimer's disease-linked presenilin mutants in human cells and mouse neurons. *Sci Signal* **3:** ra22

Cheung K-H, Shineman D, Müller M, Cárdenas C, Mei L, Yang J, Tomita T, Iwatsubo T, Lee VM-Y, Foskett JK (2008) Mechanism of Ca^{2+} disruption in Alzheimer's disease by presenilin regulation of $InsP_3$ receptor channel gating. *Neuron* **59:** 871–883

Choung SY, Kobayashi T, Takemoto K, Ishitsuka H, Inoue K (1988) Interaction of a cyclic peptide, Ro09-0198, with phosphatidylethanolamine in liposomal membranes. *Biochim Biophys Acta* **940:** 180–187

Csordas G, Varnai P, Golenar T, Roy S, Purkins G, Schneider TG, Balla T, Hajnoczky G (2010) Imaging interorganelle contacts and local calcium dynamics at the ER-mitochondrial interface. *Mol Cell* **39:** 121–132

Cupers P, Bentahir M, Craessaerts K, Orlans I, Vanderstichele H, Saftig P, De Strooper B, Annaert W (2001) The discrepancy between presenilin subcellular localization and γ-secretase processing of amyloid precursor protein. *J Cell Biol* **154:** 731–740

de Brito OM, Scorrano L (2008) Mitofusin 2 tethers endoplasmic reticulum to mitochondria. *Nature* **456:** 605–610

de Meis L, Ketzer LA, da Costa RM, de Andrade IR, Benchimol M (2010) Fusion of the endoplasmic reticulum and mitochondrial

outer membrane in rats brown adipose tissue: activation of thermogenesis by Ca^{2+}. *PLoS ONE* **5:** e9439

De Strooper B, Saftig P, Craessaerts K, Vanderstichele H, Guhde G, Annaert W, Von Figura K, Van Leuven F (1998) Deficiency of presenilin-1 inhibits the normal cleavage of amyloid precursor protein. *Nature* **391:** 387–390

Ehehalt R, Keller P, Haass C, Thiele C, Simons K (2003) Amyloidogenic processing of the Alzheimer β-amyloid precursor protein depends on lipid rafts. *J Cell Biol* **160:** 113–123

Emoto K, Kobayashi T, Yamaji A, Aizawa H, Yahara I, Inoue K, Umeda M (1996) Redistribution of phosphatidylethanolamine at the cleavage furrow of dividing cells during cytokinesis. *Proc Natl Acad Sci USA* **93:** 12867–12872

Flammang B, Pardossi-Piquard R, Sevalle J, Debayle D, Dabert-Gay AS, Thevenet A, Lauritzen I, Checler F (2012) Evidence that the amyloid-β protein precursor intracellular domain, AICD, derives from β-secretase-generated C-terminal fragment. *J Alzheimers Dis* **30:** 145–153

Foster LJ, De Hoog CL, Mann M (2003) Unbiased quantitative proteomics of lipid rafts reveals high specificity for signaling factors. *Proc Natl Acad Sci USA* **100:** 5813–5818

Fujimoto M, Hayashi T, Su TP (2012) The role of cholesterol in the association of endoplasmic reticulum membranes with mitochondria. *Biochem Biophys Res Commun* **417:** 635–639

García-Pérez C, Hajnóczky G, Csordás G (2008) Physical coupling supports the local Ca^{2+} transfer between sarcoplasmic reticulum subdomains and the mitochondria in heart muscle. *J Biol Chem* **283:** 32771–32780

Giacomello M, Drago I, Bortolozzi M, Scorzeto M, Gianelle A, Pizzo P, Pozzan T (2010) Ca^{2+} hot spots on the mitochondrial surface are generated by Ca^{2+} mobilization from stores, but not by activation of store-operated Ca^{2+} channels. *Mol Cell* **38:** 280–290

Gibson GE, Huang HM (2004) Mitochondrial enzymes and endoplasmic reticulum calcium stores as targets of oxidative stress in neurodegenerative diseases. *J Bioenerg Biomembr* **36:** 335–340

Goedert M, Spillantini MG (2006) A century of Alzheimer's disease. *Science* **314:** 777–781

Gómez-Ramos P, Asunción Morán M (2007) Ultrastructural localization of intraneuronal Aβ-peptide in Alzheimer disease brains. *J Alzheimers Dis* **11:** 53–59

Grimm MO, Grimm HS, Pätzold AJ, Zinser EG, Halonen R, Duering M, Tschäpe JA, De Strooper B, Müller U, Shen J, Hartmann T (2005) Regulation of cholesterol and sphingomyelin metabolism by amyloid-β and presenilin. *Nat Cell Biol* **7:** 1118–1123

Grimm MO, Grosgen S, Rothhaar TL, Burg VK, Hundsdorfer B, Haupenthal VJ, Friess P, Muller U, Fassbender K, Riemenschneider M, Grimm HS, Hartmann T (2011) Intracellular APP domain regulates serine-palmitoyl-CoA transferase expression and is affected in Alzheimer's disease. *Int J Alzheimers Dis* **2011:** 695413

Grimm MO, Zinser EG, Grosgen S, Hundsdorfer B, Rothhaar TL, Burg VK, Kaestner L, Bayer TA, Lipp P, Muller U, Grimm HS, Hartmann T (2012) Amyloid precursor protein (APP) mediated regulation of ganglioside homeostasis linking Alzheimer's disease pathology with ganglioside metabolism. *PLoS ONE* **7:** e34095

Hayashi T, Fujimoto M (2010) Detergent-resistant microdomains determine the localization of sigma-1 receptors to the endoplasmic reticulum-mitochondria junction. *Mol Pharmacol* **77:** 517–528

Hayashi T, Rizzuto R, Hajnoczky G, Su TP (2009) MAM: more than just a housekeeper. *Trends Cell Biol* **19:** 81–88

Heilig EA, Xia W, Shen J, Kelleher 3rd RJ (2010) A presenilin-1 mutation identified in familial Alzheimer disease with cotton wool plaques causes a nearly complete loss of γ-secretase activity. *J Biol Chem* **285:** 22350–22359

Hirai K, Aliev G, Nunomura A, Fujioka H, Russell RL, Atwood CS, Johnson AB, Kress Y, Vinters HV, Tabaton M, Shimohama S, Cash AD, Siedlak SL, Harris PL, Jones PK, Petersen RB, Perry G, Smith MA (2001) Mitochondrial abnormalities in Alzheimer's disease. *J Neurosci* **21:** 3017–3023

Hollingworth P, Harold D, Sims R, Gerrish A, Lambert J-C, Carrasquillo MM, Abraham R, Hamshere ML, Pahwa JS (2011) Common variants at *ABCA7*, *MS4A6A/MS4A4E*, *EPHA1*, *CD33* and *CD2AP* are associated with Alzheimer's disease. *Nat Genet* **43:** 429–435

Holmes O, Paturi S, Ye W, Wolfe MS, Selkoe DJ (2012) The effects of membrane lipids on the activity and processivity of purified γ-secretase. *Biochemistry* **51:** 3565–3575

Huttunen HJ, Greco C, Kovacs DM (2007) Knockdown of ACAT-1 reduces amyloidogenic processing of APP. *FEBS Lett* **581:** 1688–1692

Huttunen HJ, Peach C, Bhattacharyya R, Barren C, Pettingell W, Hutter-Paier B, Windisch M, Berezovska O, Kovacs DM (2009a) Inhibition of acyl-coenzyme A: cholesterol acyl transferase modulates amyloid precursor protein trafficking in the early secretory pathway. *FASEB J* **23:** 3819–3828

Huttunen HJ, Puglielli L, Ellis BC, MacKenzie Ingano LA, Kovacs DM (2009b) Novel N-terminal cleavage of APP precludes Aβ generation in ACAT-defective AC29 cells. *J Mol Neurosci* **37:** 6–15

Jayadev S, Leverenz JB, Steinbart E, Stahl J, Klunk W, Yu CE, Bird TD (2010) Alzheimer's disease phenotypes and genotypes associated with mutations in presenilin 2. *Brain* **133:** 1143–1154

Kim H, Ki H, Park HS, Kim K (2005) Presenilin-1 D257A and D385A mutants fail to cleave Notch in their endoproteolyzed forms, but only presenilin-1 D385A mutant can restore its γ-secretase activity with the compensatory overexpression of normal C-terminal fragment. *J Biol Chem* **280:** 22462–22472

Kimura N, Nakamura SI, Honda T, Takashima A, Nakayama H, Ono F, Sakakibara I, Doi K, Kawamura S, Yoshikawa Y (2001) Age-related changes in the localization of presenilin-1 in cynomolgus monkey brain. *Brain Res* **922:** 30–41

Kornmann B, Osman C, Walter P (2011) The conserved GTPase Gem1 regulates endoplasmic reticulum-mitochondria connections. *Proc Natl Acad Sci USA* **108:** 14151–14156

Kosicek M, Malnar M, Goate A, Hecimovic S (2010) Cholesterol accumulation in Niemann Pick type C (NPC) model cells causes a shift in APP localization to lipid rafts. *Biochem Biophys Res Commun* **393:** 404–409

Lajoie P, Nabi IR (2010) Lipid rafts, caveolae, and their endocytosis. *Int Rev Cell Mol Biol* **282:** 135–163

Leissring MA, Paul BA, Parker I, Cotman CW, LaFerla FM (1999) Alzheimer's presenilin-1 mutation potentiates inositol 1,4,5-trisphosphate-mediated calcium signaling in *Xenopus* oocytes. *J Neurochem* **72:** 1061–1068

Lingwood D, Simons K (2010) Lipid rafts as a membrane-organizing principle. *Science* **327:** 46–50

Lustbader JW, Cirilli M, Lin C, Xu HW, Takuma K, Wang N, Caspersen C, Chen X, Pollak S, Chaney M, Trinchese F, Liu S, Gunn-Moore F, Lue LF, Walker DG, Kuppusamy P, Zewier ZL, Arancio O, Stern D, Yan SS *et al* (2004) ABAD directly links Aβ to mitochondrial toxicity in Alzheimer's disease. *Science* **304:** 448–452

Macdonald JL, Pike LJ (2005) A simplified method for the preparation of detergent-free lipid rafts. *J Lipid Res* **46:** 1061–1067

Makino A, Baba T, Fujimoto K, Iwamoto K, Yano Y, Terada N, Ohno S, Sato SB, Ohta A, Umeda M, Matsuzaki K, Kobayashi T (2003) Cinnamycin (Ro 09-0198) promotes cell binding and toxicity by inducing transbilayer lipid movement. *J Biol Chem* **278:** 3204–3209

Manczak M, Anekonda TS, Henson E, Park BS, Quinn J, Reddy PH (2006) Mitochondria are a direct site of Aβ accumulation in Alzheimer's disease neurons: implications for free radical generation and oxidative damage in disease progression. *Hum Mol Genet* **15:** 1437–1449

Mandas A, Abete C, Putzu PF, la Colla P, Dessi S, Pani A (2012) Changes in cholesterol metabolism-related gene expression in peripheral blood mononuclear cells from Alzheimer patients. *Lipids Health Dis* **11:** 39

Marambaud P, Shioi J, Serban G, Georgakopoulos A, Sarner S, Nagy V, Baki L, Wen P, Efthimiopoulos S, Shao Z, Wisniewski T, Robakis NK (2002) A presenilin-1/γ-secretase cleavage releases the E-cadherin intracellular domain and regulates disassembly of adherens junctions. *EMBO J* **21:** 1948–1956

Marki F, Hanni E, Fredenhagen A, van Oostrum J (1991) Mode of action of the lanthionine-containing peptide antibiotics duramycin, duramycin B and C, and cinnamycin as indirect inhibitors of phospholipase A2. *Biochem Pharmacol* **42:** 2027–2035

Mattson MP (2010) ER calcium and Alzheimer's disease: in a state of flux. *Sci Signal* **3:** pe10

McMillan PJ, Leverenz JB, Dorsa DM (2000) Specific downregulation of presenilin 2 gene expression is prominent during early

stages of sporadic late-onset Alzheimer's disease. *Brain Res Mol Brain Res* **78:** 138–145

Morohashi Y, Kan T, Tominari Y, Fuwa H, Okamura Y, Watanabe N, Sato C, Natsugari H, Fukuyama T, Iwatsubo T, Tomita T (2006) C-terminal fragment of presenilin is the molecular target of a dipeptidic γ-secretase-specific inhibitor DAPT (N-[N-(3,5-difluorophenacetyl)-L-alanyl]-S-phenylglycine t-butyl ester. *J Biol Chem* **281:** 14670–14676

Morrow IC, Parton RG (2005) Flotillins and the PHB domain protein family: rafts, worms and anaesthetics. *Traffic* **6:** 725–740

Myhill N, Lynes EM, Nanji JA, Blagoveshchenskaya AD, Fei H, Simmen KC, Cooper TJ, Thomas G, Simmen T (2008) The subcellular distribution of calnexin is mediated by PACS-2. *Mol Biol Cell* **19:** 2777–2788

Naj AC, Jun G, Beecham GW, Wamg L-S, Vardarajan BN, Buros J, Gallins PJ, Buxbaum JD, Jarvik GP, Crane PK, Larson EB (2011) Common variants at *MS4A4/MS4A6E*, *CD2AP*, *CD33* and *EPHA1* are associated with late-onset Alzheimer's disease. *Nat Genet* **43:** 436–441

Nesic I, Guix FX, Vennekens K, Michaki V, Van Veldhoven PP, Feiguin F, De Strooper B, Dotti CG, Wahle T (2012) Alterations in phosphatidylethanolamine levels affect the generation of Aβ. *Aging Cell* **11:** 63–72

Pani A, Dessì S, Diaz G, La Colla P, Abete C, Mulas C, Angius F, Cannas MD, Orru CD, Cocco PL, Mandas A, Putzu P, Laurenzana A, Cellai C, Costanza AM, Bavazzano A, Mocali A, Paoletti F (2009a) Altered cholesterol ester cycle in skin fibroblasts from patients with Alzheimer's disease. *J Alzheimers Dis* **18:** 829–841

Pani A, Mandas A, Diaz G, Abete C, Cocco PL, Angius F, Brundu A, Mucaka N, Pais ME, Saba A, Barberini L, Zaru C, Palmas M, Putzu F, Mocali A, Paoletti F, La Colla P, Dessi S (2009b) Accumulation of neutral lipids in peripheral blood mononuclear cells as a distinctive trait of Alzheimer patients and asymptomatic subjects at risk of disease. *BMC Med* **7:** 66–77

Pasternak SH, Bagshaw RD, Guiral M, Zhang S, Ackerley CA, Pak BJ, Callahan JW, Mahuran DJ (2003) Presenilin-1, nicastrin, amyloid precursor protein, and γ-secretase activity are co-localized in the lysosomal membrane. *J Biol Chem* **278:** 26687–26694

Peterson C, Goldman JE (1986) Alterations in calcium content and biochemical processes in cultured skin fibroblasts from aged and Alzheimer donors. *Proc Natl Acad Sci USA* **83:** 2758–2762

Pettegrew JW, Panchalingam K, Hamilton RL, McClure RJ (2001) Brain membrane phospholipid alterations in Alzheimer's disease. *Neurochem Res* **26:** 771–782

Pimplikar SW (2009) Reassessing the amyloid cascade hypothesis of Alzheimer's disease. *Int J Biochem Cell Biol* **41:** 1261–1268

Pottekat A, Menon AK (2004) Subcellular localization and targeting of N-acetylglucosaminyl phosphatidylinositol de-N-acetylase, the second enzyme in the glycosylphosphatidylinositol biosynthetic pathway. *J Biol Chem* **279:** 15743–15751

Pratico D, Delanty N (2000) Oxidative injury in diseases of the central nervous system: focus on Alzheimer's disease. *Am J Med* **109:** 577–585

Puglielli L, Ellis BC, Ingano LA, Kovacs DM (2004) Role of acyl-coenzyme A:cholesterol acyltransferase activity in the processing of the amyloid precursor protein. *J Mol Neurosci* **24:** 93–96

Puglielli L, Konopka G, Pack-Chung E, Ingano LA, Berezovska O, Hyman BT, Chang TY, Tanzi RE, Kovacs DM (2001) Acyl-coenzyme A:cholesterol acyltransferase modulates the generation of the amyloid β-peptide. *Nat Cell Biol* **3:** 905–912

Puglielli L, Tanzi RE, Kovacs DM (2003) Alzheimer's disease: the cholesterol connection. *Nature Neurosci* **6:** 345–351

Risselada HJ, Marrink SJ (2008) The molecular face of lipid rafts in model membranes. *Proc Natl Acad Sci USA* **105:** 17367–17372

Rusinol AE, Cui Z, Chen MH, Vance JE (1994) A unique mitochondria-associated membrane fraction from rat liver has a high capacity for lipid synthesis and contains pre-Golgi secretory proteins including nascent lipoproteins. *J Biol Chem* **269:** 27494–27502

Sano R, Annunziata I, Patterson A, Moshiach S, Gomero E, Opferman J, Forte M, d'Azzo A (2009) GM1-ganglioside accumulation at the mitochondria-associated ER membranes links ER stress to Ca^{2+}-dependent mitochondrial apoptosis. *Mol Cell* **36:** 500–511

Sato N, Imaizumi K, Manabe T, Taniguchi M, Hitomi J, Katayama T, Yoneda T, Morihara T, Yasuda Y, Takagi T, Kudo T, Tsuda T, Itoyama Y, Makifuchi T, Fraser PE, St George-Hyslop P, Tohyama M (2001) Increased production of β-amyloid and vulnerability to endoplasmic reticulum stress by an aberrant spliced form of presenilin 2. *J Biol Chem* **276:** 2108–2114

Schon EA, Area-Gomez E (2010) Is Alzheimer's disease a disorder of mitochondria-associated membranes? *J Alzheimers Dis* **20:** S281–S292

Schon EA, Przedborski S (2011) Mitochondria: the next (neurode)-generation. *Neuron* **70:** 1033–1053

Shen J, Kelleher 3rd RJ (2007) The presenilin hypothesis of Alzheimer's disease: evidence for a loss-of-function pathogenic mechanism. *Proc Natl Acad Sci USA* **104:** 403–409

Simons K, Vaz WL (2004) Model systems, lipid rafts, and cell membranes. *Annu Rev Biophys Biomol Struct* **33:** 269–295

Sorice M, Manganelli V, Matarrese P, Tinari A, Misasi R, Malorni W, Garofalo T (2009) Cardiolipin-enriched raft-like microdomains are essential activating platforms for apoptotic signals on mitochondria. *FEBS Lett* **583:** 2447–2450

Stefani M, Liguri G (2009) Cholesterol in Alzheimer's disease: unresolved questions. *Curr Alzheimer Res* **6:** 15–29

Stieren E, Werchan WP, El Ayadi A, Li F, Boehning D (2010) FAD mutations in amyloid precursor protein do not directly perturb intracellular calcium homeostasis. *PLoS ONE* **5:** e11992

Stutzmann GE, Smith I, Caccamo A, Oddo S, Laferla FM, Parker I (2006) Enhanced ryanodine receptor recruitment contributes to Ca^{2+} disruptions in young, adult, and aged Alzheimer's disease mice. *J Neurosci* **26:** 5180–5189

Su B, Wang X, Bonda D, Perry G, Smith M, Zhu X (2010) Abnormal mitochondrial dynamics-a novel therapeutic target for Alzheimer's disease? *Mol Neurobiol* **41:** 87–96

Szabadkai G, Bianchi K, Varnai P, De Stefani D, Wieckowski MR, Cavagna D, Nagy AI, Balla T, Rizzuto R (2006) Chaperone-mediated coupling of endoplasmic reticulum and mitochondrial Ca^{2+} channels. *J Cell Biol* **175:** 901–911

Thinakaran G, Harris CL, Ratovitski T, Davenport F, Slunt HH, Price DL, Borchelt DR, Sisodia SS (1997) Evidence that levels of presenilins (PS1 and PS2) are coordinately regulated by competition for limiting cellular factors. *J Biol Chem* **272:** 28415–28422

Todaro GJ, Green H (1963) Quantitative studies of the growth of mouse embryo cells in culture and their development into established lines. *J Cell Biol* **17:** 299–313

Uemura K, Farner KC, Nasser-Ghodsi N, Jones P, Berezovska O (2011) Reciprocal relationship between APP positioning relative to the membrane and PS1 conformation. *Mol Neurodegener* **6:** 15

Urano Y, Hayashi I, Isoo N, Reid PC, Shibasaki Y, Noguchi N, Tomita T, Iwatsubo T, Hamakubo T, Kodama T (2005) Association of active γ-secretase complex with lipid rafts. *J Lipid Res* **46:** 904–912

Vance JE (1990) Phospholipid synthesis in a membrane fraction associated with mitochondria. *J Biol Chem* **265:** 7248–7256

Vance JE (2003) Molecular and cell biology of phosphatidylserine and phosphatidylethanolamine metabolism. *Prog Nucl Acid Res Mol Biol* **75:** 69–111

Vance JE (2008) Phosphatidylserine and phosphatidylethanolamine in mammalian cells: two metabolically related aminophospholipids. *J Lipid Res* **49:** 1377–1387

Vetrivel KS, Cheng H, Kim SH, Chen Y, Barnes NY, Parent AT, Sisodia SS, Thinakaran G (2005) Spatial segregation of γ-secretase and substrates in distinct membrane domains. *J Biol Chem* **280:** 25892–25900

Vetrivel KS, Cheng H, Lin W, Sakurai T, Li T, Nukina N, Wong PC, Xu H, Thinakaran G (2004) Association of γ-secretase with lipid rafts in post-Golgi and endosome membranes. *J Biol Chem* **279:** 44945–44954

Voelker DR (2005) Bridging gaps in phospholipid transport. *Trends Biochem Sci* **30:** 396–404

Walther TC, Farese Jr. RV (2009) The life of lipid droplets. *Biochim Biophys Acta* **1791:** 459–466

Wang X, Su B, Zheng L, Perry G, Smith MA, Zhu X (2009) The role of abnormal mitochondrial dynamics in the pathogenesis of Alzheimer's disease. *J Neurochem* **109:** 153–159

Wells K, Farooqui AA, Liss L, Horrocks LA (1995) Neural membrane phospholipids in Alzheimer disease. *Neurochem Res* **20:** 1329–1333

Williamson CD, Zhang A, Colberg-Poley AM (2011) The human cytomegalovirus protein UL37 exon 1 associates with internal lipid rafts. *J Virol* **85:** 2100–2111

Winkler E, Kamp F, Scheuring J, Ebke A, Fukumori A, Steiner H (2012) Generation of Alzheimer disease-associated $A\beta_{42/43}$ by γ-secretase can directly be inhibited by modulation of membrane thickness. *J Biol Chem* **287:** 21326–21334

Yu G, Nishimura M, Arawaka S, Levitan D, Zhang L, Tandon A, Song YQ, Rogaeva E, Chen F, Kawarai T, Supala A, Levesque L, Yu H, Yang DS, Holmes E, Milman P, Liang Y, Zhang DM, Xu DH, Sato C *et al* (2000) Nicastrin modulates presenilin-mediated *notch/glp-1* signal transduction and βAPP processing. *Nature* **407:** 48–54

Yuyama K, Yanagisawa K (2010) Sphingomyelin accumulation provides a favorable milieu for GM1 ganglioside-induced assembly of amyloid β-protein. *Neurosci Lett* **481:** 168–172

Zampese E, Fasolato C, Kipanyula MJ, Bortolozzi M, Pozzan T, Pizzo P (2011) Presenilin 2 modulates endoplasmic reticulum (ER)-mitochondria interactions and Ca^{2+} cross-talk. *Proc Natl Acad Sci USA* **108:** 2777–2782

Zheng YZ, Berg KB, Foster LJ (2009) Mitochondria do not contain lipid rafts, and lipid rafts do not contain mitochondrial proteins. *J Lipid Res* **50:** 988–998